*The Canadian Mineralogist*
Vol. 35, pp. 627-658 (1997)

# CHARACTERIZATION OF MULTIPLE FLUID-FLOW EVENTS AND RARE-EARTH-ELEMENT MOBILITY ASSOCIATED WITH FORMATION OF UNCONFORMITY-TYPE URANIUM DEPOSITS IN THE ATHABASCA BASIN, SASKATCHEWAN

MOSTAFA FAYEK*

*Department of Earth and Planetary Sciences, University of New Mexico, Albuquerque, New Mexico 87131, U.S.A.*

T. KURTIS KYSER

*Department of Geological Sciences, Queen's University, Kingston, Ontario K7L 3N6*

## ABSTRACT

The Proterozoic Athabasca Basin in northern Saskatchewan is host to the world's largest and richest uranium deposits. Three main stages of uranium mineralization have been identified on the basis of cross-cutting relationships, textures observed in thin section and by SEM, oxygen and U–Pb isotopic compositions, and chemical compositions. All three stages of uranium mineralization have been variably altered to becquerelite, calcio-uranoite, and coffinite. U–Pb chemical ages and $^{207}Pb/^{206}Pb$ ages of uranium mineralization indicate that the three main uranium-deposition events occurred at ~1500 Ma during peak diagenesis, at 950 Ma, and as late as 300 Ma. Stage-1 and -2 uraninite and pitchblende have the lowest $\delta^{18}O$ values, which range from –32 to –19.5‰, whereas stage-3 uraninite has $\delta^{18}O$ values near –10‰. The alteration minerals becquerelite, calcio-uranoite, and coffinite have $\delta^{18}O$ values near 0‰. $^{87}Sr/^{86}Sr$ ratios of uranium minerals strongly reflect the proportion of basin and basement fluid involved in the formation of the deposits. Uranium minerals entirely hosted by basement rocks have relatively low $^{87}Sr/^{86}Sr$ ratios, which indicate that the majority of the fluid involved in the formation of these deposits was basinal brine, whereas the relatively high $^{87}Sr/^{86}Sr$ ratios of uranium minerals partially hosted by the overlying sandstones indicate that a high proportion of the Sr and by inference, the fluid involved in the formation of these deposits was derived from the basement rocks. High concentrations of *REE*-rich hydrothermal fluorapatite, crandallite-group minerals, and xenotime are associated with uranium mineralization in the Athabasca Basin. In addition, the uranium minerals have up to 12,000 ppm total *REE* contents and are *HREE*-enriched. The relations among *REE*-rich minerals, diagenetic clays and uranium mineralization in the basin and basement rocks indicate extensive *REE* mobility during diagenesis of the Athabasca Basin. The *REE* and U most likely were derived from detrital fluorapatite and zircon in the sandstone, garnet in the basement and, to a lesser extent, diagenetic clay minerals and zircon in basement rocks. The *REE*, and possibly the uranium, were likely transported as F-complexes. The high concentration of uranium (427 million kg) and *REE* in deposits of the Athabasca Basin render unconformity-type deposits viable sources of *REE* as well as uranium, and demonstrate that *REE* mobility can be extreme in certain geological environments.

*Keywords:* uraninite, oxygen isotopes, $^{87}Sr/^{86}Sr$ ratios, $^{207}Pb/^{206}Pb$ ages, rare-earth elements, alteration, Athabasca Basin, Saskatchewan.

## SOMMAIRE

Le bassin d'Athabasca, dans le nord du Saskatchewan, d'âge protérozoïque, est le site des gisements d'uranium les plus volumineux et les plus riches du monde. Trois stades de minéralisation ont été identifiés selon les critères de terrain, les textures étudiées en lame mince, les observations au microscope électronique à balayage, les mesures isotopiques (oxygène, U–Pb) et les compositions chimiques. À chaque stade, il y a eu altération d'intensité variable en un assemblage de becquerelite, calcio-uranoïte et coffinite. D'après les âges "chimiques" U–Pb et les datations $^{207}Pb/^{206}Pb$, les stades importants de déposition de l'uranium ont eu lieu à environ 1500 Ma, au cours des réactions de diagenèse, à 950 Ma, et encore beaucoup plus récemment, à environ 300 Ma. L'uraninite et la pitchblende des stades 1 et 2 montrent les valeurs les plus faibles de $\delta^{18}O$, entre –32 et –19.5‰, tandis que l'uraninite du stade 3 montre une valeur de $\delta^{18}O$ près de –10‰. Les minéraux secondaires (becquerelite, calcio-uranoïte et coffinite) ont une valeur de $\delta^{18}O$ proche de 0‰. Les rapports $^{87}Sr/^{86}Sr$ des minéraux uranifères dépendent fortement de la proportion dans la phase fluide de composantes issues du bassin et du socle. Les minéraux d'uranium situés dans les roches du socle ont un rapport $^{87}Sr/^{86}Sr$ relativement faible, ce qui indique que la majeure partie de la phase fluide qui a causé ces gisements avait une origine dans le bassin sédimentaire. En revanche, les valeurs relativement élevées de $^{87}Sr/^{86}Sr$ des minéraux uranifères en partie encaissés

[1] Present address: Department of Geological Sciences, Queen's University, Kingston, Ontario K7L 3N6.
**E-mail address*: fayek@geol.queensu.ca

dans les grès sus-jacents montrent qu'une fraction importante du Sr, et par extension la phase fluide impliquée dans la formation de ces gisements, ont été dérivées des roches du socle. Des quantités importantes d'apatite hydrothermale riche en terres rares, de minéraux du groupe de la crandallite et de xénotime sont associées aux zones minéralisées en uranium. De plus, les minéraux d'uranium contiennent jusqu'à 12,000 ppm de terres rares, et sont enrichis en terres rares lourdes. Les interrelations parmi les minéraux riches en terres rares, les argiles diagénétiques et le minerai uranifère des roches du bassin et du socle indiquent une mobilisation importante des terres rares au cours de la diagenèse des roches du bassin d'Athabasca. Les terres rares et l'uranium ont tout probablement été dérivés à partir de la fluorapatite et le zircon détritiques des grès, le grenat des roches du socle, et à degré moindre, les argiles diagénétiques et le zircon des roches du socle. Les terres rares, et peut-être l'uranium, auraient été mobilisés sous forme de complexes fluorés. La concentration élevée d'uranium ($427 \times 10^6$ kg) et de terres rares des gisements du bassin d'Athabasca les rendent des sources viables de terres rares aussi bien que d'uranium, et démontrent que dans certains milieux géologiques, la mobilité des terres rares peut être extrême.

(Traduit par la Rédaction)

*Mots-clés:* uraninite, isotopes d'oxygène, rapports $^{87}Sr/^{86}Sr$, âges $^{207}Pb/^{206}Pb$, terres rares, altération, bassin d'Athabasca, Saskatchewan.

## INTRODUCTION

The Proterozoic Athabasca Basin, in northern Saskatchewan, is host to some of the world's largest and richest uranium deposits (Fig. 1a). Uranium mineralization was first discovered in the early 1950s in vein-type deposits along the northern shore of Lake Athabasca, and by the late 1960s, unconformity-type uranium deposits were discovered (Cumming & Krstic 1992). At present, the Athabasca Basin has an estimated geological reserve of 427 million kg of $U_3O_8$ (Uranium Saskatchewan 1994). These high-grade deposits occur within 500 meters of the surface, at or near the unconformity between the Athabasca Group sandstones and the Aphebian metamorphic and igneous rocks of the Hearne Province. Their accessibility and high grade make these deposits attractive exploration targets; Saskatchewan has become a major producer (30%) of the world's uranium. By the late 1980s, high concentrations of rare-earth elements (*REE*) were discovered to be associated with unconformity-type uranium mineralization (Fryer & Taylor 1987, Quirt *et al.* 1991, Fayek & Kyser 1993). Uraninite and pitchblende ($UO_2$ + Th + *REE*), which are the most abundant uranium ore minerals in the Athabasca Basin, have *REE* contents of up to 12,000 ppm, implying that the total geological reserve of *REE* in the Athabasca Basin is *ca.* 5 million kg. In addition, *REE* phosphate minerals are present in trace amounts in every sandstone formation of the Helikian Athabasca Group in the Athabasca Basin (Wilson 1985).

Unconformity-type uranium deposits have been studied extensively, and a multitude of models have been proposed to explain their genesis. Initial hypotheses were based on an erosional model, in view of the proximity of the ore to the unconformity (Langford 1974, Knipping 1974). More recently, investigators have suggested that large-scale movement of fluid and diagenesis within the Athabasca Group sandstones were largely responsible for the transport and deposition of uranium (Hoeve & Sibbald 1978, Hoeve *et al.* 1980). In a recent modification of the diagenetic-hydrothermal model, uranium transport and deposition are linked to regional-scale fluid-flow hydrodynamics, large-scale structures, time–temperature profiles, fluid mixing, and geochemical conditions that existed within the Athabasca Basin (Hoeve & Quirt 1984, Wilson & Kyser 1987, Kyser *et al.* 1988, 1990, Kotzer & Kyser 1993, 1995). Geochronological, petrographic, and isotopic studies of uranium minerals (Dyck 1978, Baadsgaard *et al.* 1984, Cumming & Krstic 1992, Kotzer & Kyser 1993) illustrate the difficulties associated with establishing the age of initial emplacement of the uranium, the fluids responsible for uranium transport and deposition, and the source of the uranium, because uraninite and pitchblende are extremely soluble in an oxidizing environment. These minerals, therefore, are geochemically unstable in most surficial environments, and are susceptible to later alteration by meteoric fluids (Dyck 1978, Baadsgaard *et al.* 1984, Kotzer & Kyser 1995).

The objectives of this study are to document the effects of alteration on the texture, chemistry, oxygen isotopic composition, and U–Pb, $^{87}Sr/^{86}Sr$, and $^{207}Pb/^{206}Pb$ isotope systematics of uranium ore, in order to determine the timing of fluid-flow events associated with uranium mineralization. In addition, the *REE* content and the characteristics of the uranium mineralization and rocks within the basin are used to determine the probable source of *REE* and U, and the mechanism by which the *REE* were transported and concentrated.

## GEOLOGICAL CONSIDERATIONS

The Athabasca Basin formed as a series of NE–SW-oriented sub-basins (Fig. 1b) at ~1700–1750 Ma (Armstrong & Ramaekers 1985, Kotzer & Kyser 1992, 1995). Sub-basin formation was controlled by major NE–SW Hudsonian-age faults rooted in underlying Aphebian metasediments and Archean gneisses. The Athabasca Basin consists of sequences of Helikian polycyclic, mature, fluvial to marine quartz-rich sandstone, collectively referred to as the Athabasca Group (Fig. 1c), which were deposited in a near-shore, shallow-shelf

environment (Ramaekers & Dunn 1977, Ramaekers 1981). The Archean gneisses and Aphebian metasediments are separated from the overlying Athabasca Group sediments by a well-developed unconformity and associated paleosol. The paleosol beneath the unconformity generally extends for several meters, within which the basement gneisses are strongly altered to illite, hematite, kaolinite and chlorite (Hoeve & Quirt 1984). The Hudsonian-age faults are major crustal lineaments that intersect the overlying sequence of sandstone and have remained intermittently active to recent times (Hoeve & Quirt 1984).

The basal sequence of the Athabasca Group (Manitou Falls and Fair Point formations) consists of permeable coarse- to fine-grained, and hematite-rich conglomerates and silty sandstones (Fig. 1c). In the Manitou Falls

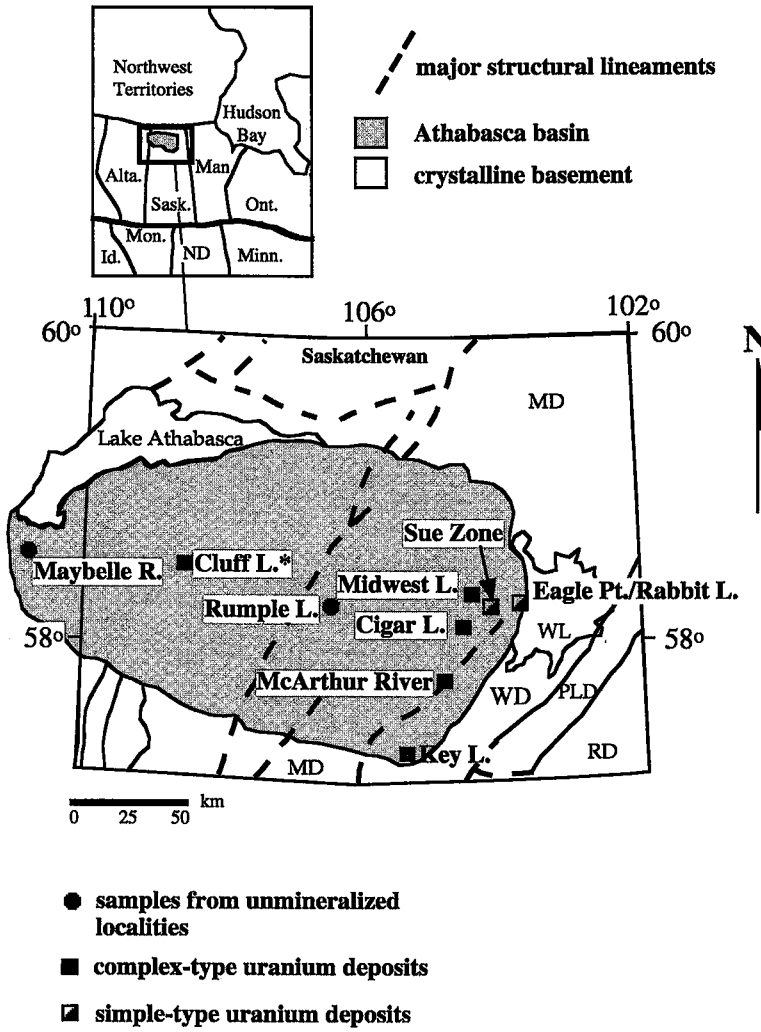


FIG. 1a. Map showing the extent of the Athabasca Basin, location of the uranium deposits and unmineralized localities where samples were collected, and major lithostructural domains in the crystalline basement of Saskatchewan (modified from Hoeve & Sibbald 1978). * Unmineralized sandstone samples were collected from drill-core near Cluff Lake (*i.e.*, CSP8, C8, C2). Abbreviations: MD: Mudjatik Domain, WD: Wollaston Domain, PLD: Peter Lake Domain, RD: Rottenstone Domain, and WL: Wollaston Lake, R: River, L: Lake.

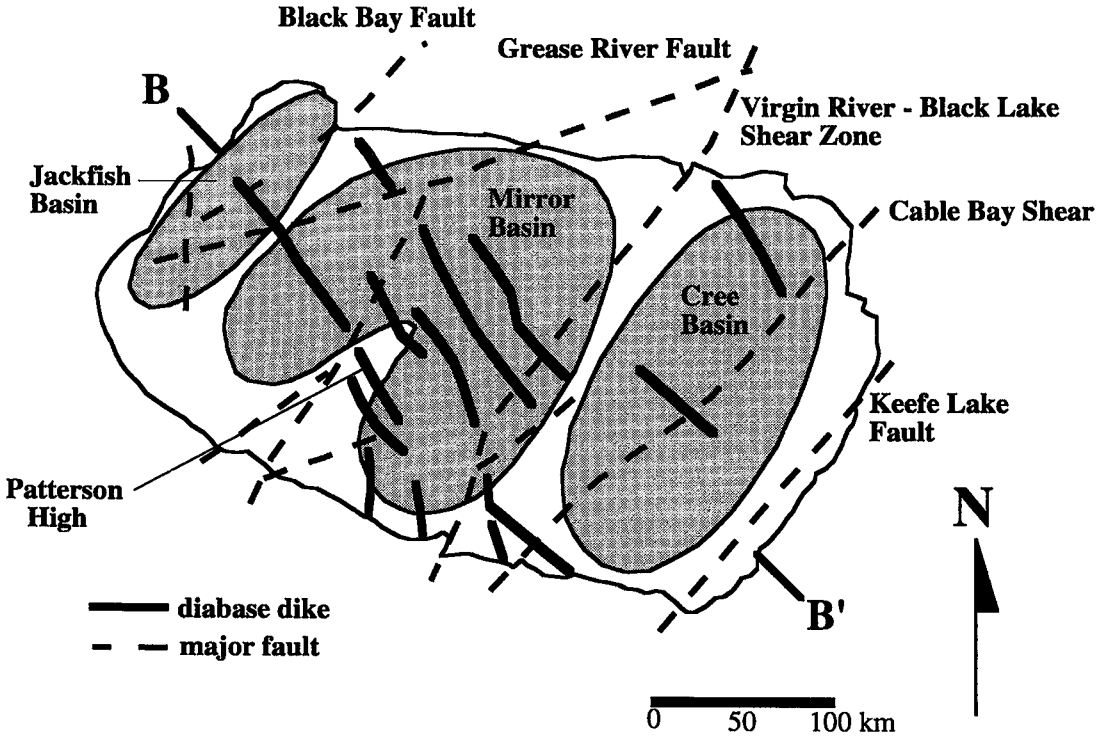


FIG. 1b. Map showing the location of sub-basins, major faults and diabase dikes in the Athabasca Basin (modified from Hoeve & Quirt 1984).

Formation, hematite is disseminated along thin stratigraphic horizons, indicating local oxidation of heavy mineral suites. These bands of heavy minerals occur mainly near the basal portion of the Manitou Falls Formation and less so in the Locker Lake Formation. The basal sandstones are overlain by an arkosic succession of less-permeable marine sandstones, phosphatic (fluorapatite) siltstones, and phosphatic mudstones (the Lazenby Lake, Wolverine Point, Locker Lake, Otherside and Tuma Lake formations, respectively), which are in turn overlain by shales (Douglas Formation) and stromatolitic dolomite (Carswell Formation).

The Aphebian metasedimentary rocks and Archean gneisses that comprise the basement are members of the Wollaston Domain of the Trans-Hudson Orogen (Lewry & Sibbald 1977, 1980, Lewry *et al.* 1985, MacDonald 1987). The Aphebian metasedimentary rocks unconformably overlie the Archean granitoid gneisses and consist typically of quartz, plagioclase, biotite, cordierite, ± garnet and tourmaline, with several anatectic and graphitic layers (Ey *et al.* 1991, Marlatt *et al.* 1992). Individual quartzite units occur locally and are generally separated by intervals of garnet–cordierite gneiss (Marlatt *et al.* 1992).

The Athabasca Group rocks are cut by a series of northwest-trending mafic dykes, which were emplaced along reactivated fractures during post-Athabasca tectonic activity (1350–900 Ma) (Ey *et al.* 1991). The dykes are believed to be related to the Mackenzie dyke swarm (Cumming & Krstic 1992). The Athabasca Basin is presently 1 to 2 km thick; however, temperature estimates derived from fluid inclusions indicate that the sedimentary sequence may have reached a thickness of 5–7 km during the mid-Proterozoic (Pagel *et al.* 1980).

Diagenesis of the Athabasca Basin produced highly saline (>100 000 mg/L), oxidizing, uranium-bearing fluids (basinal brines) that interacted with the Athabasca sandstones and formed basin-wide assemblages of clay and silicate minerals at temperatures of *ca.* 200°C (Kotzer & Kyser 1995). The Aphebian metasedimentary and Archean granitoid rocks were affected by chemically and isotopically distinct, reducing, "basement" fluids (Kotzer & Kyser 1995). Hudsonian-age faults that intersected the unconformity focussed the flow of the basement fluids, and where these fluids mixed with the basinal fluids, deposition of uranium-bearing minerals occurred. Associated with these, high-angle reverse-fault structures, at most unconformity-type uranium deposits,

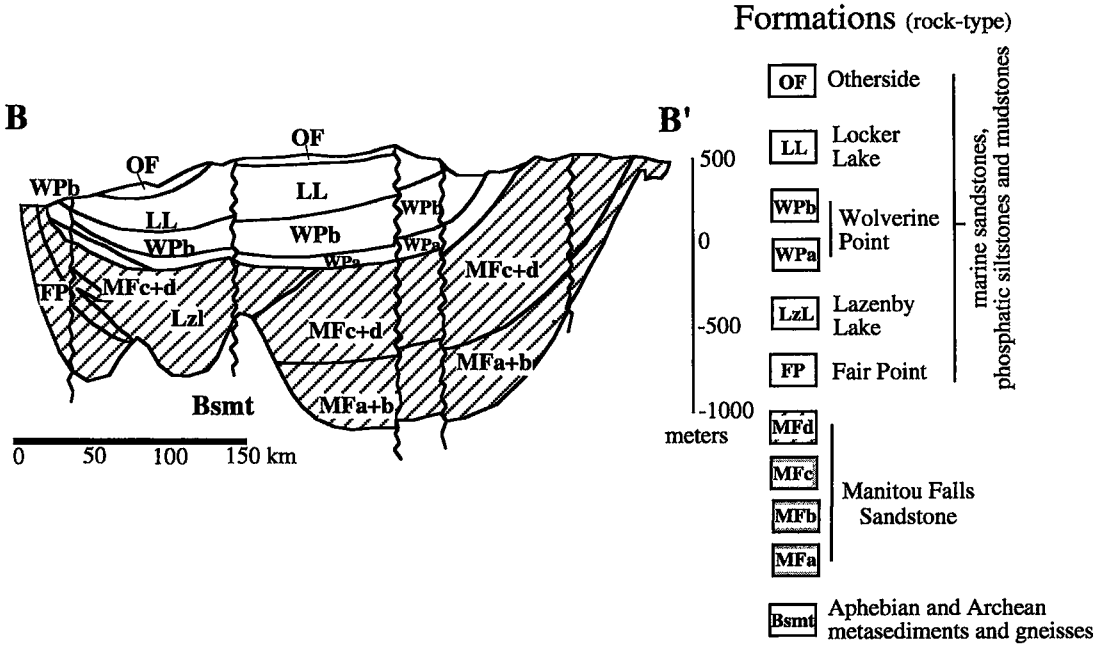


FIG. 1c. Cross-section along B–B′ showing the general stratigraphy of the Athabasca Basin (modified from Hoeve & Quirt 1984).

are graphite-rich gneisses and pelites, which provided a structural, rather than chemical control on the deposition of uranium (Kyser *et al.* 1988).

On the basis of the spatial association of uranium ore with the unconformity and the sulfide mineral assemblage associated with uranium mineralization, two distinct types of unconformity-type uranium deposits have been identified in the Athabasca Basin. Uranium deposits formed at the unconformity, hosted partially by sandstone, are referred to as complex-type deposits because Ni–Co–As–Fe–Cu–Pb sulfides and arsenides are associated with uranium minerals. The abundance of sulfides and arsenides indicates that uranium deposition occurred under reducing conditions, in which a large volume of basement fluid interacted with the oxidizing basinal brine. In contrast, uranium deposits hosted entirely within fractures in basement rocks are referred to as simple-type deposits, with trace amounts of sulfides and arsenides associated with the uranium mineralization. The lack of sulfides implies that these deposits may have formed under less reducing conditions, wherein reduction of the oxidizing basinal brine occurred during interaction with the basement rocks, with minimal contribution of a basement fluid. Intense hydrothermal alteration in the sandstone and basement gneisses and metasediments surrounding the uranium deposits led to a large halo of illitized sandstone and local enrichments of K, Mg, Ca, B, U, Ni, Co, As, Cu, and Fe (Hoeve *et al.* 1980, Wallis *et al.* 1983, Bruneton 1993, Kotzer & Kyser 1990a, 1995). Extensive areas of silicification associated with dravite, kaolinite and chlorite are found near some deposits (Marlatt *et al.* 1992).

## SAMPLING PROCEDURES AND ANALYTICAL TECHNIQUES

Drill-core samples were collected for stable and radiogenic isotopic and geochemical analyses from six high-grade uranium deposits located along the eastern margin of the Athabasca Basin (Fig. 1a). Samples were chosen from areas of high-grade uranium mineralization, alteration halos associated with uranium mineralization, and unmineralized Manitou Falls sandstone and basement rocks proximal to uranium mineralization. Unmineralized samples from various formations of the Athabasca Group Sandstones, and basement rocks, also were collected from Rumple Lake, the Cluff Lake area, and the Maybelle River project (Fig. 1a). Samples collected from the central and western regions of the Athabasca Basin, barren of uranium mineralization, represent background samples. Polished thin sections of samples collected from drill core were prepared to determine the paragenetic relations among primary and secondary uranium-bearing and *REE*-bearing minerals.

The mineralogical characteristics of the uranium and *REE* minerals were examined using reflected and transmitted light microscopy, back-scattered electron imaging (BSE), and scanning electron microscopy (SEM). Chemical compositions of the uranium oxides and *REE* minerals were determined by wavelength-dispersion spectroscopy (WDS) using a fully automated JEOL JXA–8600 X-ray micro-analyzer at an operating voltage 20 keV, a beam diameter of 2 μm, and counting times of 40 s per element. Concentrations of volatile elements (*i.e.*, Na) were established first in the sequence of analyses. Detection limits of the elements were on the order of 0.1 wt%. The ZAF data-reduction package was used for the various elements.

Primary and secondary uranium minerals were sampled for O, Pb, and Sr isotopic analyses, and for *REE* determinations, using a micro-drill (*ca.* 100 μm diameter). Sample purity was verified optically and by X-ray diffraction. Oxygen was liberated from the uranium oxide minerals using the $BrF_5$ technique of Clayton & Mayeda (1963) and converted to $CO_2$. The oxygen isotopic compositions are reported in units of ‰ relative to Standard Mean Ocean Water (SMOW) and were measured on the Finnigan Mat Delta and 251 gas source mass spectrometers, at the University of Saskatchewan. Replicate analyses for $\delta^{18}O$ are reproducible to ± 0.2‰; using this technique, the $\delta^{18}O$ value of NIST–28 quartz is 9.6‰.

Unmineralized sandstone samples and samples collected from the alteration halo associated with uranium mineralization were prepared for *REE* and trace-element analyses using conventional agate mill crushing and dissolution techniques; uranium oxide minerals were digested using conventional techniques (Xie *et al.* 1994). However, one-week digestion periods were required. Selected samples were redigested using the $Na_2O_2$ sinter method (Robinson *et al.* 1986, Longerich *et al.* 1990), and these results were found to be comparable to those using the HF-based dissolution. Samples were analyzed using a Perkin Elmer Sciex Elan 5000 inductively coupled plasma mass spectrometer (ICP–MS) under standard operating conditions (Xie *et al.* 1994). Strontium was separated from the solutions using Sr-spec chromatographic material, and Pb was separated using standard-column separation techniques described by Parrish *et al.* (1987). Fractions were analyzed on a Finnigan Mat 261 multi-collector mass spectrometer, at the University of Saskatchewan. Replicate analyses of NIST–987 Sr standard and NIST–982 Pb standard gave mean values for $^{87}Sr/^{86}Sr$ of 0.710243 ± 0.000010 ($n$=10) and for $^{207}Pb/^{206}Pb$ of 0.46708 ± 0.00022 ($n$=10), respectively. The Pb isotopic data were reduced using the program ISOPLOT (Ludwig 1993). U–Pb chemical ages of uranium mineral grains were calculated from the U, Th and Pb contents determined from electron-microprobe data using the method described by Bowles (1990). The accuracy of Pb analyses by the electron microprobe is ±0.1%, which is equivalent to errors of 10 Ma for chemical ages. The volume of the Athabasca Basin was calculated using the formula:

$$V = \int_b^a \pi[f(x)]_2\, dx$$

where $a = 0$, $b = 200$, $f(x) = 3.3x$.

## Petrographic Relations and Mineral Paragenesis

### *Clay and silicate minerals*

A detailed paragenesis of clay and silicate minerals (Fig. 2) was developed for the entire basin by Kotzer & Kyser (1992, 1995) using petrographic relations, stable and radiogenic isotope compositions, and analyses of fluid inclusions in altered sandstones and metasedimentary rocks proximal to, and distal from, unconformity-type uranium deposits. Early diagenesis of the Athabasca Basin produced quartz overgrowths (Q1) and hematite (H1) on detrital quartz, and oxidation of ilmenite to specular hematite (H1) and rutile (R1) in laterally extensive detrital bands of heavy minerals (Kotzer & Kyser 1992, 1995). The sandstones presently consist of *ca.* 95% detrital quartz and 5% secondary minerals by volume. The suite of heavy minerals also includes detrital tourmaline with an overgrowth of dravite (T1), which appears optically and chemically identical to hydrothermal dravite (T1) found in alteration halos associated with uranium mineralization, and interstitial dravite (T1) associated with early illite (I1) in altered and brecciated sandstone. A basin-wide mineral assemblage consisting of variable proportions of illite (I1) and kaolinite (K1) was produced by the alteration of detrital silicates during peak diagenesis of the Athabasca Group sediments. Areas proximal to faults and fractures, which focussed fluid flow, are hydrothermally altered. Hydrothermal alteration consists dominantly of illite (I1), intergrown with euhedral quartz (Q2) and dravite (T1, T2), Al–Mg-bearing chlorite (C2), and hematite (H2), with varying amounts of uraninite (U1, U2) (Fig. 2). Hydrothermal alteration is largely contemporaneous with the basin-wide clay-mineral assemblage and postdates the early overgrowths of quartz (Q1). In the vicinity of hydrothermally altered fault-zones, which are intensely fractured owing to repeated reactivation, early-formed diagenetic and hydrothermal minerals are altered and overprinted by late fluids that formed blocky kaolinite in vugs (K2) and fractures (K3).

In metasedimentary rocks and in overlying sandstones proximal to the unconformity throughout the basin, rosettes of trioctahedral chlorite or clinochlore (C1) infill pore spaces. However, varying amounts of dioctahedral chlorite or sudoite (C2) occur in hydrothermally altered sandstones and metasedimentary rocks of the basement near unconformity-type uranium deposits and fault zones that intersect the unconformity (Hoeve &

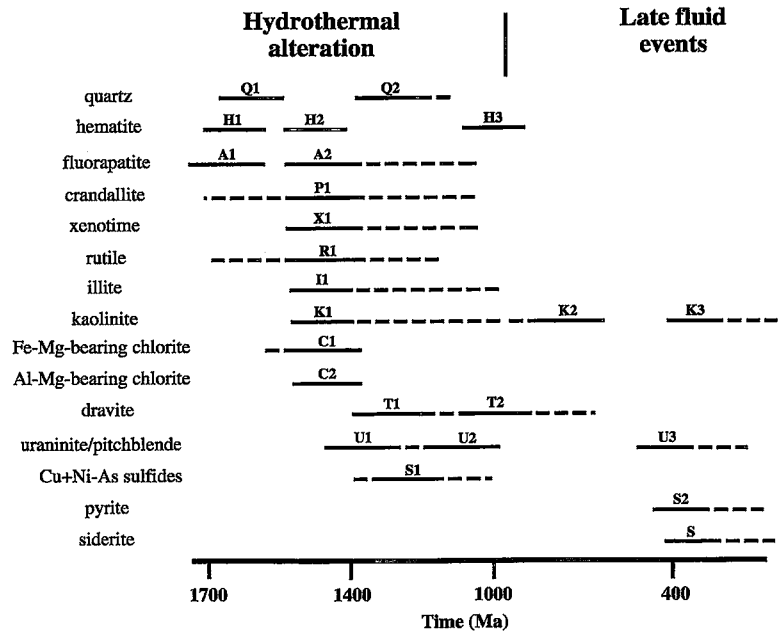


FIG. 2. Fluid–mineral–age relationships of various minerals throughout the Athabasca Basin (modified from Kotzer & Kyser 1995). Letters refer to specific generations of minerals described in text.

Quirt 1984, Wilson & Kyser 1987, Kotzer & Kyser 1995). Sudoite also occurs in fault zones up to 300 m above the unconformity, suggesting that these faults allowed fluid to upwell to much higher stratigraphic levels (Kotzer & Kyser 1995).

*Uranium minerals*

In hand specimens from each deposit, uraninite and its botryoidal variety pitchblende are the most common uranium ore minerals. They occur as black to dark gray masses with a metallic to submetallic luster. The ore is highly fractured, with sulfides, arsenides, clay and rust-colored carbonate minerals infilling fractures. Uraninite occurs as cubes ranging in size from 0.5 cm to 3 cm, and in massive form. Pitchblende occurs as nodular masses that range in size from 1 to 5 cm across.

Three main stages of ore formation are observed in thin section and by BSE. These are: stage-1 (U1) and -2 (U2) uraninite and pitchblende, and stage-3 uraninite (U3). All stages of uranium ore are variably altered to Ca-rich, hydrous uranium minerals ("gummite") and coffinite.

Stage-1 uraninite occurs as homogeneous masses and euhedral crystals that exhibit the highest reflectivity and earliest paragenesis (Fig. 3a). Pitchblende occurs as nodular masses that attain several cm across (Fig. 3b). Nodules are composed of many botroids that exhibit a radial texture as a result of uniformly distributed radial shrinkage-cracks. Spaces between botroids are filled with clay minerals and Ni–Cu arsenides (S1). Stage-1 uraninite and pitchblende are characterized by high Pb contents (13.47–25.32 wt% PbO), low Si and Ca contents (<3 wt% $SiO_2$, CaO) and very low Fe contents (<1.5 wt% FeO). Variation in Pb, Si and Ca contents, and chemical ages (Table 1, Fig. 4) likely reflect cryptic alteration by subsequent fluids that affected virtually all stage-1 uranium mineralization.

Stage-2 uranium mineralization also includes massive pitchblende and uraninite (Fig. 3c). Associated with the stage-2 uranium minerals are Ni–Cu arsenides and Ni–Co sulfarsenides (S1). Stage-2 uranium minerals are characterized by intermediate Pb contents (6.45–11.98 wt% PbO), intermediate Si and Ca contents (1–3 wt% $SiO_2$, CaO), relatively high Fe contents (~1 wt% FeO) and intermediate U–Pb chemical ages (Table 1, Fig. 4).

Stage-3 uranium mineralization occurs as massive uraninite (Fig. 3d) and as uraninite in fractures. Uraninite appears unaltered, is highly reflective, and is characterized by low to moderate Pb contents (0.67–5.54 wt% PbO), variable Si, Ca, and Fe contents, and chemical ages less than 500 Ma (Fig. 4). Cu–Fe sulfides (S2) are commonly associated with stage-3 uraninite. Stage-3 massive uraninite, with a high reflectivity and concordant

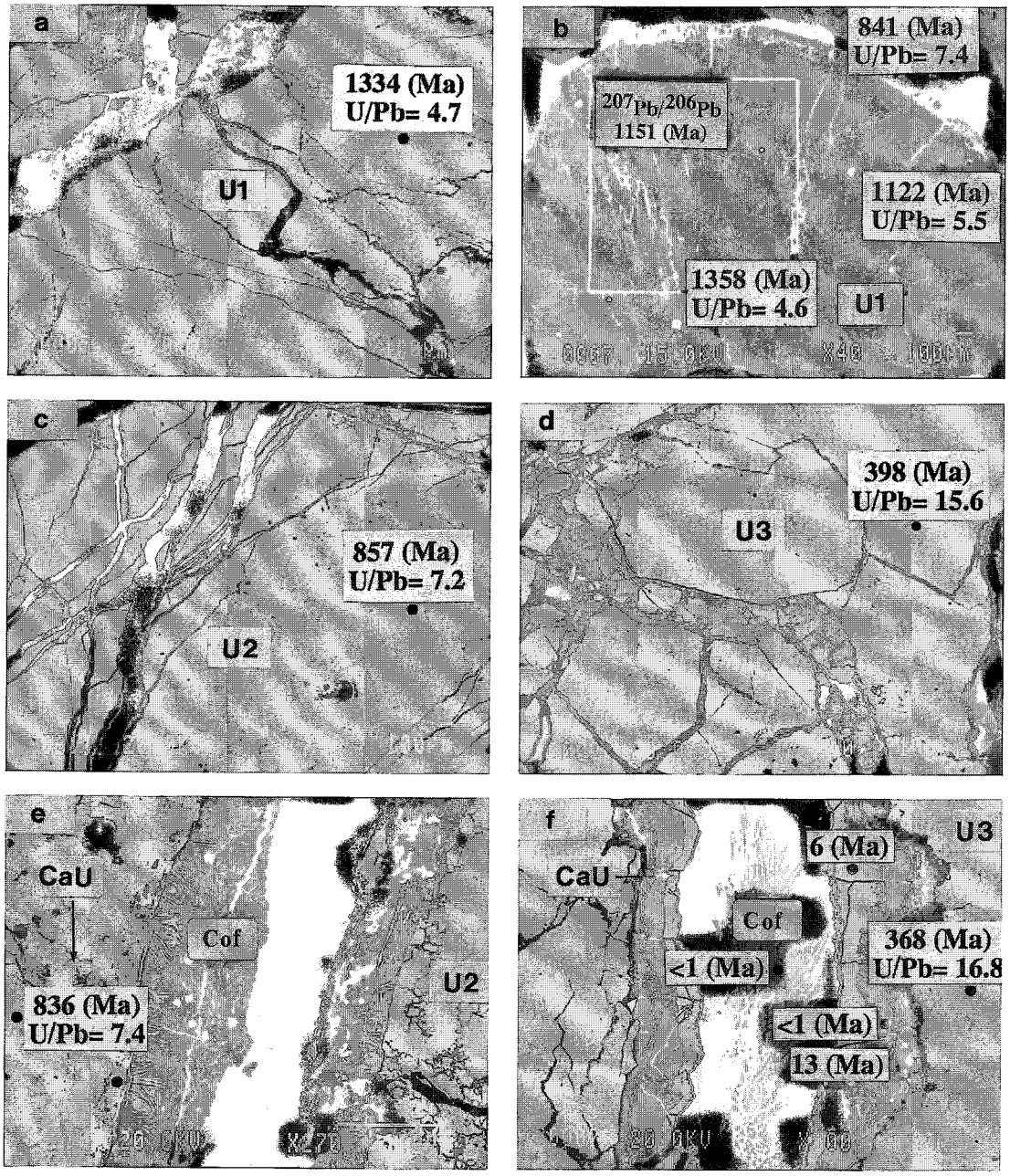


FIG. 3. Back-scattered electron photographs of the three dominant stages of uranium minerals, "gummite" and coffinite from unconformity-type deposits of the Athabasca Basin. Chemical ages and U/Pb ratios from electron-microprobe analyses are indicated. a) Sample from McArthur River (204–503) showing unaltered high-reflectance stage-1 uraninite (U1). b) Sample from the Sue Zone (528–95) showing a botryoid of stage-1 pitchblende (U1) with radial fractures and decreasing U–Pb chemical age from the center to the rim. The box represents the sample area for $^{207}Pb/^{206}Pb$ analyses. c) Sample from McArthur River (236–515) showing optically pristine stage-2 uraninite (U2). d) Sample from Cigar Lake (480–176) showing optically pristine stage-3 uraninite (U3) with "gummite" and coffinite infilling fractures. e) Sample from McArthur River (236–515) showing "gummite" (CaU), coffinite (Cof), and stage-2 uraninite (U2) proximal to a carbonate microveinlet (black). f) Sample from Cigar Lake (480–176) showing colloform bands of "gummite" (CaU) and coffinite (grey), feathery coffinite (Cof), and stage-3 uraninite (U3) proximal to a carbonate vein (black).

TABLE 1. MINERALOGICAL AND CHEMICAL COMPOSITION OF URANIUM MINERALS*, AND CHEMICAL U–Pb AGES OF UNCONFORMITY-TYPE URANIUM MINERALIZATION FROM THE ATHABASCA BASIN

| Sample No. (DDH/depth) | Remarks | $U_3O_8$ | $SiO_2$ | CaO | PbO | FeO | Chemical U-Pb Age (Ma**) |
|---|---|---|---|---|---|---|---|
| McArthur R.: | | | | | | | |
| 204-503 | stage-1 uran/pitch | 83.54-93.21 | 0.09-0.49 | 0-1.23 | 13.40-16.46 | 0.12-1.27 | 1056-1334 |
| | stage-2 pitch | 86.26 | 0.48 | 1.32 | 8.48 | 1.27 | 668 |
| | Ca-U hydrate | 66.22 | 1.99 | 4.84 | 8.21 | 2.09 | 842 |
| 229-534 | stage-2 uran | 86.82-87.25 | 0.62-0.63 | 1.44-1.47 | 10.87-11.54 | 0.63-0.73 | 846-903 |
| | Ca-U hydrate | 84.93 | 3.85 | 2.80 | 2.44 | 2.51 | 195 |
| 230-528 | stage-1 uran | 84.67-85.50 | 0.25 | 0 | 15.15-15.37 | 0.21-0.22 | 1210-1230 |
| 236-511 | stage-1 uran/pitch | 85.20-86.85 | 0.19-1.12 | 0 | 13.62-14.33 | 0.11-0.13 | 1065-1142 |
| | stag-3 uran | 91.04-93.21 | 0.77-1.12 | 1.22-1.45 | 3.71-4.80 | 0.13-0.19 | 271-358 |
| | Ca-U hydrate | 94.16 | 1.61 | 2.81 | 0.15 | 0.26 | 11 |
| 236-515 | stage-2 uran/pitch | 86.99-88.69 | 0.45-0.66 | 0.90-1.73 | 9.57-11.08 | 0.43-0.62 | 733-857 |
| | Ca-U hydrate | 85.51-87.52 | 0.63-0.68 | 2.71-7.75 | 0.89-9.10 | 0.21-0.56 | 69-723 |
| | coffinite | 72.12 | 14.99 | 5.84 | 0.08 | 0 | 8 |
| Cigar L.: | | | | | | | |
| 480-176 | stage-3 uran | 91.49-94.08 | 0.37-1.84 | 0.94-2.93 | 2.10-5.36 | 0.08-0.68 | 161-398 |
| | Ca-U hydrate | 85.13-91.29 | 2.80-4.05 | 2.33-3.96 | 0-1.00 | 0.14-0.44 | <1-74 |
| | coffinite | 70.84-78.91 | 15.06-16.26 | 0.14-2.84 | 0-0.14 | 0.06-0.10 | <1-13 |
| Key L.: | | | | | | | |
| 470-6 | Ca-U hydrate | 80.71-82.91 | 1.90-2.38 | 3.30-3.57 | 0.26-1.25 | 1.49-1.79 | 22-103 |
| 470-10-7 | stage-1 pitch | 77.06-78.09 | 0.22-0.24 | 0.89-1.22 | 19.10-19.25 | 0.24-0.37 | 1661-1769 |
| | Ca-U hydrate | 72.49-76.49 | 2.10-3.80 | 2.16-3.78 | 3.21-5.75 | 0.14-0.17 | 285-539 |
| 478-14 | stage-1 pitch | 76.89-78.94 | 0.25-0.47 | 0.96-1.23 | 17.58-20.31 | 0.33-0.38 | 1512-1794 |
| | Ca-U hydrate | 65.25-77.07 | 2.83-6.64 | 2.38-4.83 | 1.74-5.81 | 0.96-1.80 | 160-549 |
| Midwest L.: | | | | | | | |
| 576-193 | stage-1 pitch | 79.41-80.99 | 0.15-0.44 | 0.88-1.55 | 14.63-18.30 | 0.20-0.36 | 1227-1565 |
| | coffinite | 69.78-74.20 | 10.70-12.50 | 0.80-0.89 | 4.88-5.65 | 0.13-0.16 | 12 |
| 576-191 | stage-1 pitch | 77.18-79.13 | 0.20-0.29 | 0.70-1.18 | 18.35-20.14 | 0.16-0.64 | 1588-1772 |
| | coffinite | 70.33-73.51 | 10.93-15.35 | 1.06-1.76 | 5.36-11.37 | 0.05-0.07 | 518-1050 |
| 581-190 | stage-1 pitch | 76.72-81.10 | 0.11-0.19 | 0.36-1.14 | 16.86-25.32 | 0.19-0.25 | 1412-2009 |
| | stage-2 uran/pitch | 85.25 | 0.82 | 1.35 | 7.76 | 0.20 | 618 |
| | stage-3 uran | 86.34 | 1.39 | 1.39 | 5.13 | 0.21 | 403 |
| | coffinite | 62.48-66.41 | 15.16-19.31 | 1.00-2.13 | 3.07-10.78 | 0-0.06 | 332-1106 |
| Sue Zone: | | | | | | | |
| 211-136 | stage-3 uran | 94.3 | 2.46 | 0 | 1.88 | 0.14 | 135 |

TABLE 1. CONT' D

| Sample No. (DDH/depth) | Remarks | $U_3O_8$ | $SiO_2$ | CaO | PbO | FeO | Chemical U-Pb Age (Ma**) |
|---|---|---|---|---|---|---|---|
| 247 | stage-1 uran | 83.11-84.11 | 0.20-0.24 | 0.21-0.41 | 15.41-17.38 | 0.23-0.28 | 1244-1420 |
| | Ca-U hydrate | 78.11-85.25 | 4.72-6.67 | 3.04-5.07 | 0-1.25 | 0.33-0.74 | <1-145 |
| | coffinite | 61.40-66.85 | 9.74-11.93 | 0.51-0.72 | 4.25-4.39 | 0.09-0.12 | 446-470 |
| 528-95 | stage-1 uran | 79.95-81.48 | 0.20-0.46 | 1.31-1.98 | 13.47-15.99 | 0.25-0.33 | 1123-1358 |
| | stage-2 uran/pitch | 74.92-84.67 | 0.34-2.82 | 0.66-2.31 | 6.45-11.23 | 0.04-0.50 | 519-952 |
| | stage-3 uran | 78.56-83.54 | 2.18-3.65 | 0.61-1.61 | 0.67-1.41 | 0-0.26 | 54-122 |
| 528-129 | stage-1 uran/pitch | 74.44-78.34 | 0.08-0.32 | 1.23-2.70 | 15.96-22.32 | 0.10-0.48 | 1403-2063 |
| Eagle Pt. North: | | | | | | | |
| H277-49 | stage-2 uran/pitch | 83.11-84.61 | 0.56-1.20 | 1.18-2.17 | 7.39-11.17 | 0.12-0.33 | 593-913 |
| | Ca-U hydrate | 76.80-79.02 | 2.35-3.60 | 3.97-5.23 | 4.63-5.33 | 0.06-0.16 | 409-458 |
| H779-57 | stage-2 uran/pitch | 81.94-84.41 | 0.51-1.41 | 1.14-2.08 | 7.30-11.98 | 0.19-0.33 | 705-938 |
| Eagle Pt. South: | | | | | | | |
| 213-213 | stage-2 uran/pitch | 83.39-85.06 | 0.59-0.87 | 1.35-1.66 | 7.30-9.86 | 0.10-0.15 | 588-803 |
| | stage-3 uran | 84.30-86.52 | 1.49-1.55 | 0.92-1.28 | 4.12-5.54 | 0.08-0.11 | 326-446 |
| | Ca-U-hydrate | 72.36 | 4.07 | 3.74 | 2.73 | 0.61 | 256 |
| | coffinite | 48.64 | 12.68 | 2.82 | 1.51 | 1.17 | 211 |
| 213-224 | stage-2 uran/pitch | 80.64-82.66 | 0.53-2.65 | 1.30-1.83 | 7.14-10.23 | 0.09-0.19 | 601-854 |
| | coffinite | 58.57 | 15.90 | 2.27 | 2.45 | 1.18 | 284 |

Note: all values are quoted in wt%. Abbreviations: uran: uraninite, pitch: pitchblende, DDH: diamond drill hole, L.: Lake, R.: River, Pt.: Point. Depth is reported in meters. * Range in chemical composition expresses variations in samples analyzed. ** Ages calculated using the equation $t = (Pb*10^{10}\ yr)/(1.612\ U + 4.95Th)$ (Bowles 1990).

U–Pb ages (Kotzer & Kyser 1993), may represent the introduction of new ore, or the complete recrystallization of previously deposited ore.

"Gummite", which is ubiquitous in each deposit, is yellow to orange and occurs as microveinlets that cut across uraninite and pitchblende. In thin section, "gummite" occurs as homogeneous colloform bands along the edge of pitchblende botroids and uraninite grains proximal to carbonate veins, or as microveinlets that cut across the common uranium ore minerals (Fig. 3e). On the basis of U/Ca ratio and the classification proposed by Smith (1984) and Burns *et al.* (1996), the "gummite" consists of becquerelite and calcio-uranoite. These minerals are characterized by moderate reflectivities, low Pb contents (0–9.10 wt% PbO), moderate but variable Si and Fe contents, and relatively high Ca contents (2.16–7.75 wt% CaO; Table 1, Fig. 5).

Coffinite, in hand specimen, occurs as grey-black microveinlets. In thin section, it occurs as colloform bands along uraninite grains and pitchblende botroids (Fig. 3e), and as feathery dark grey crystalline masses in carbonate veins (Fig. 3f). Coffinite is characterized by a very low reflectivity, low Pb contents (0–11.37 wt% PbO), moderate but variable Ca and Fe contents, and high Si contents (9.74–19.31 wt% $SiO_2$; Table 1, Fig. 5).

*REE-rich silicates and phosphates*

Detailed petrographic and electron-microprobe studies of the sandstone and basement rocks near mineralization, from barren localities, and from the alteration halos associated with uranium mineralization, were conducted to determine the host of the *REE* associated with uranium mineralization. Barren sandstone contains trace

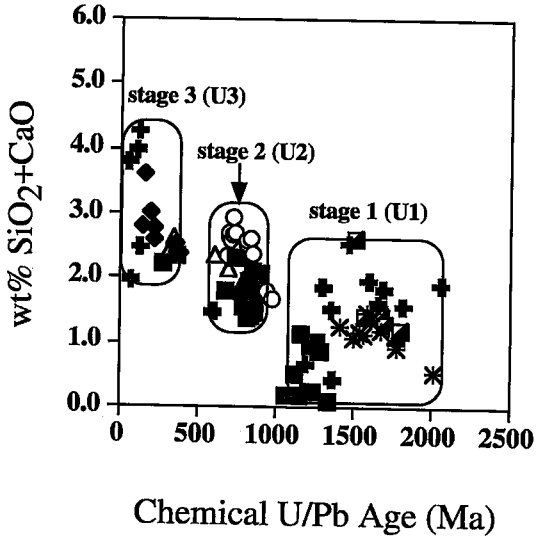


FIG. 4. Relationship between $SiO_2$ + CaO contents and chemical U–Pb ages of stage-1, -2 and -3 uraninite and pitchblende from the Athabasca Basin (data from Table 1). Symbols: ■ McArthur River, ◆ Cigar Lake, ○ Eagle Point North, △ Eagle Point South, ✚ Sue Zone, ✳ Midwest Lake, ◪ Key Lake.

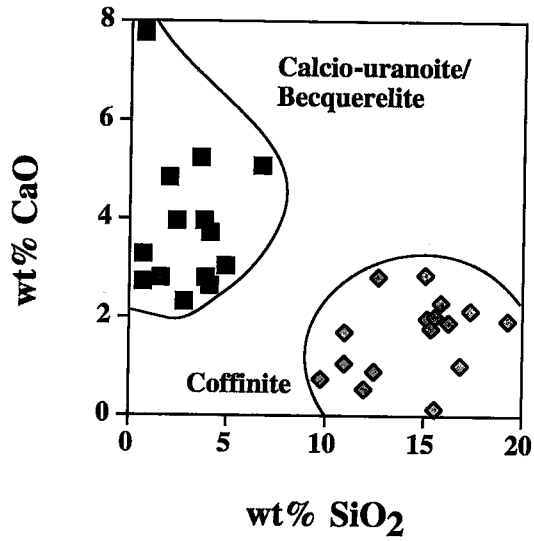


FIG. 5. Relationship between $SiO_2$ and CaO for "gummite" (■) and coffinite (◈) from unconformity-type deposits from the Athabasca Basin (data from Table 1).

amounts of detrital fluorapatite and zircon (Figs. 6a, b), and minor amounts of a diagenetic crandallite-group phase (P1), rutile (R1) and hematite (H1). Detrital fluorapatite and zircon are subhedral, occur mainly within the detrital quartz grains (Figs. 6a, b), and rarely as detrital interstitial minerals, indicating that they may have been removed by fluids flowing through the sandstone. Electron-microprobe analyses indicate that the detrital fluorapatite contains up to 4.92 wt% F (Table 2, Fig. 7a).

The crandallite-group phase is a solid solution between crandallite [$CaAl_3(PO_4)OH_5$] and goyazite [$SrAl_3(PO_4)OH_5$], and is euhedral in shape (Fig. 6c). It fills interstitial space between detrital quartz grains (Fig. 6d) and is associated with the diagenetic overgrowths of quartz, indicating it is a paragenetically early phase in the evolution of the basin. The crandallite-group mineral commonly occurs as irregular masses intermixed with blades of rutile and hematite (Fig. 6e). Electron-microprobe analyses of the crandallite-group mineral indicate high Al (~15 wt% $Al_2O_3$) and low F (~0.5 wt%) contents (Table 2). Quirt *et al.* (1991) reported the presence of minor amounts of unaltered detrital monazite, and early-diagenetic fluorapatite (A1) cements have been observed in the Wolverine Point Formation (Hoeve & Quirt 1984). An abundance of the crandallite-group mineral and xenotime (Fig. 6f) is associated with the hydrothermal clay and silicate minerals that comprise the alteration halo associated with uranium mineralization.

Basement rocks near zones of mineralization are intensely altered. Detrital zircon is pseudomorphically replaced by xenotime (XI; Figs. 6f, g, h). Xenotime also occurs along fractures within, and as an overgrowth around, zircon (Figs. 6g, h). In addition, there is an abundance of hydrothermal fluorapatite (A2; Figs. 6i, j) and the crandallite-group mineral (P1; Fig. 6f). Almandine garnet in basement rocks, which has a small amount of the grossular component, is replaced (Fig. 6j) by hydrothermal fluorapatite (A2) and Al–Mg-bearing chlorite (C2). Hydrothermal fluorapatite occurs as irregular aggregates and as small (~100 μm) euhedral grains enriched in P and Ca relative to detrital fluorapatite (Fig. 8). The crandallite-group phase from the alteration halo occurs as irregular masses and fine euhedral grains (~1 μm; Fig. 6f), and is enriched in F relative to the diagenetic crandallite-group mineral from the sandstones, whereas the crandallite-group mineral from basement rocks contains intermediate F contents and variable Al contents (Figs. 7b, c). Electron-microprobe analyses of detrital zircon, and unaltered and altered crystals of zircon from the alteration halo and basement rocks (Table 3), indicate that altered zircon containing discrete zones of xenotime (Figs. 6g, h), is enriched in Y, P, U, $H_2O$ and, to a lesser extent, Al, and depleted in Si relative to unaltered and detrital grains of zircon (Figs. 9a, b, c). Inferred $H_2O$ contents of altered hydrated zircon are as high as 10 wt% (Table 3).

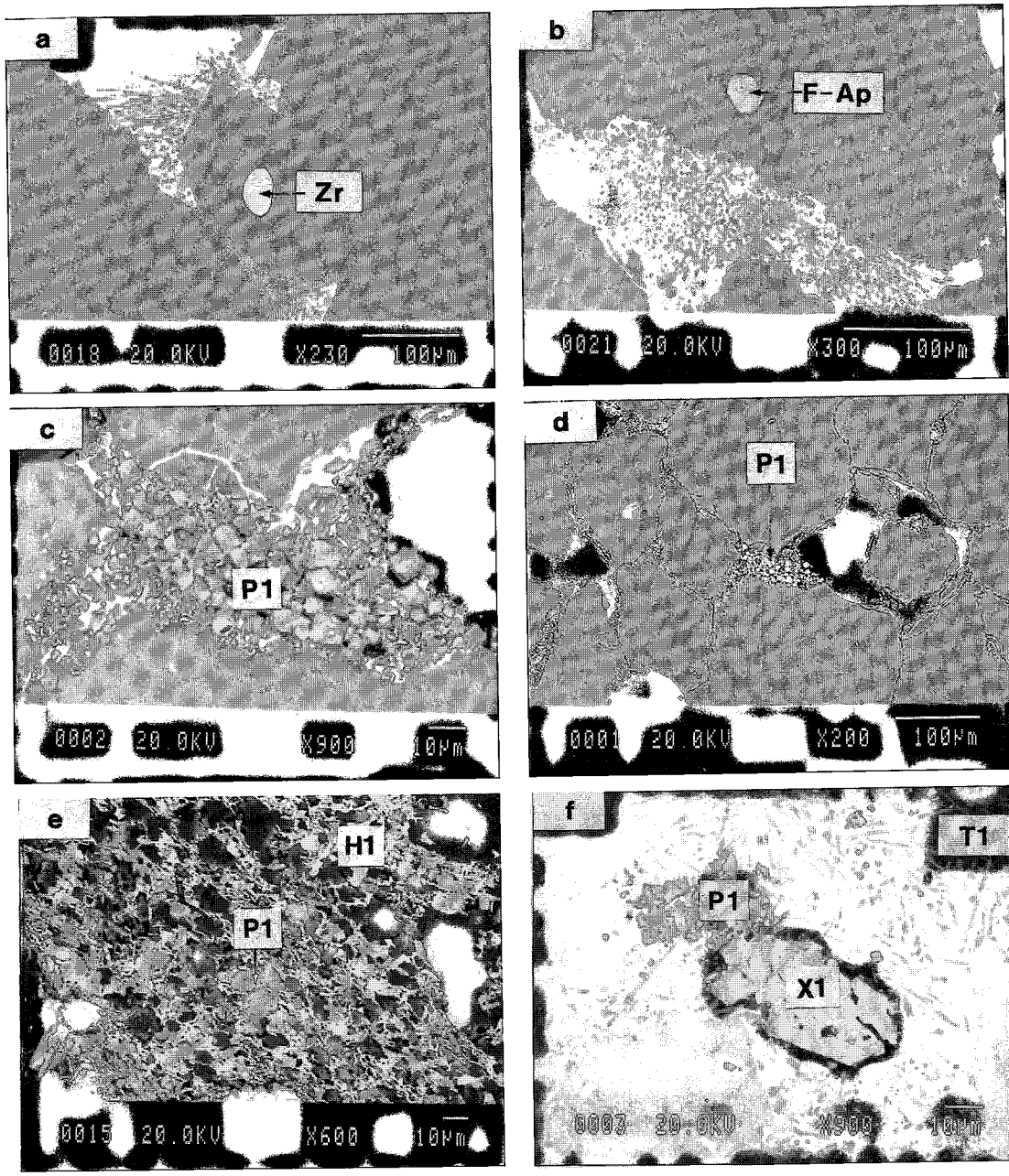


FIG. 6. Back-scattered electron photographs of phosphate, silicate and oxide minerals from samples of unmineralized sandstone, the alteration halo associated with uranium minerals, and basement rocks from the Athabasca Basin. a) Sample from McArthur River (204–154) of sandstone away from mineralization showing a relatively unaltered grain of detrital zircon (Zr) in detrital quartz. b) Sample from McArthur River (204–154) of sandstone away from mineralization showing a relatively unaltered detrital grain of fluorapatite (F–Ap) in detrital quartz. c) Sample from west-central portion of the Basin, near Cluff Lake (C2–120), of barren sandstone showing euhedral crandallite-group minerals (P1). d) Sample from west-central portion of the Basin, near Cluff Lake (C2–120), of barren sandstone showing euhedral crystals of crandallite-group mineral (P1) infilling interstitial space between detrital quartz grains. e) Sample from Rumple Lake (RL1–1192), of barren sandstone showing irregular masses of the crandallite-group mineral (P1) intermixed with hematite (H1). f) Sample from McArthur River (204–526), from the alteration halo associated with uranium minerals, showing xenotime (X1) pseudomorphically replacing zircon, and irregular masses of goyazite (P1) associated with dravite (T1).

→

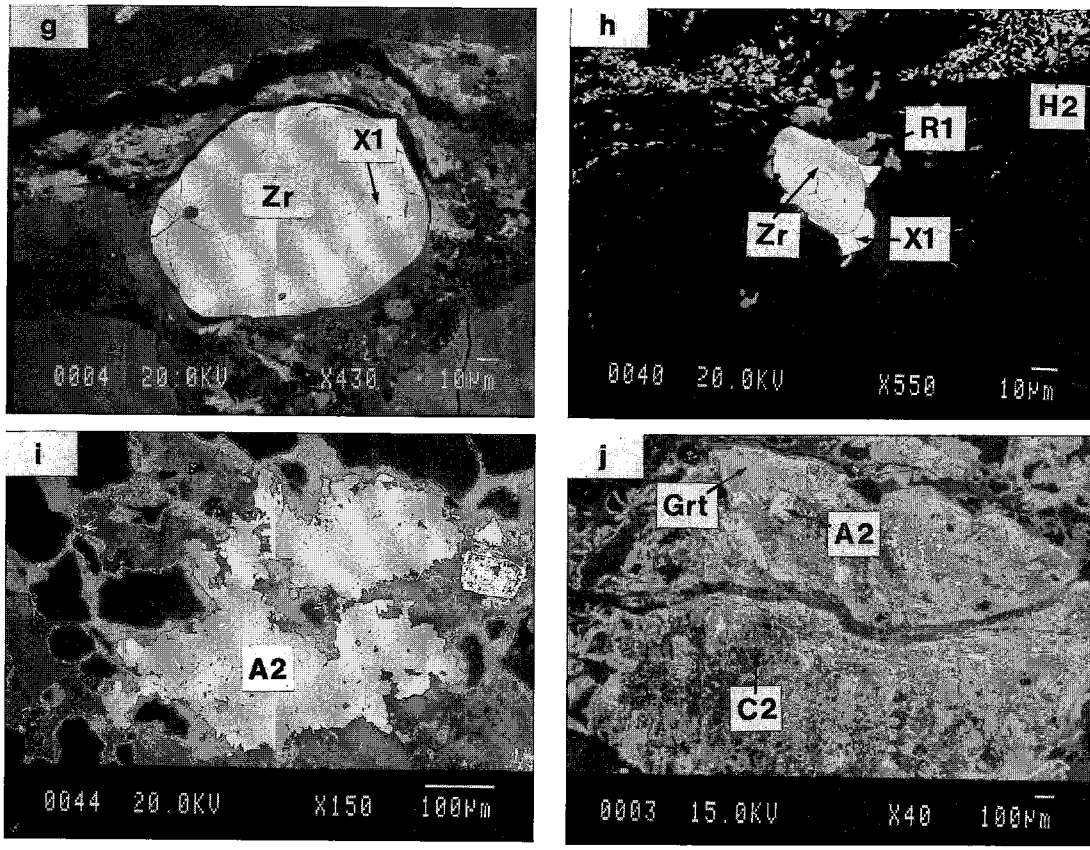


FIG. 6 (cont'd). g) Sample from McArthur River (204–635), of basement rocks showing the alteration of zircon (Zr) to xenotime (X1) along fractures and growth zones. h) Sample from McArthur River (178–563), of basement rocks showing alteration of zircon (Zr) with an overgrowth of xenotime (X1) associated with rutile (R1) and hematite (H2). i) Sample from McArthur River (204–635), of basement rocks showing massive hydrothermal fluorapatite (A2). j) Sample from McArthur River (204–635) showing altered almandine-rich garnet (Grt), hydrothermal fluorapatite (A2), and Al–Mg-bearing chlorite (C2).

## AGE, OXYGEN AND Sr ISOTOPIC COMPOSITION OF URANIUM MINERALIZATION

### *U–Pb chemical age*

Electron-microprobe data on the U, Th and Pb content of uranium minerals may be used to calculate a chemical age for the mineral. The chemical age is derived from the assumption that the total lead present in the sample is of radiogenic origin and a result of the decay of U and Th, and that the mineral has not lost or acquired lead since the time of crystallization. The advantage of this method lies in the ability to make *in situ* measurements to provide dates related to mineralogical features (Bowles 1990).

Chemical ages of the three stages of uranium mineralization, "gummite" and coffinite were calculated based on their U and Pb content. Stage-1 uraninite, as expected, has the oldest ages, ranging from 1056 to 2063 Ma. Stage-2 pitchblende has ages ranging from 519 to 968 Ma, whereas stage-3 uraninite has ages that range from 54 to 446 Ma. "Gummite" and coffinite usually have low and variable Pb contents, so that the U–Pb chemical ages for these alteration minerals are normally young, but highly inaccurate.

From each stage of mineralization, uranium minerals that have the highest reflectivities and are least altered according to their chemical compositions generally have the oldest ages. The wide range in ages for each stage of uranium mineralization most likely reflects variable alteration by subsequent fluids that interacted with the uranium minerals.

Clay minerals and paleomagnetic directions associated with, and postdating, uranium mineralization from

TABLE 2. REPRESENTATIVE RESULTS OF ELECTRON-MICROPROBE ANALYSES OF PHOSPHATE MINERALS FROM UNMINERALIZED SANDSTONE, ALTERATION ENVELOPE ASSOCIATED WITH URANIUM MINERALS, AND BASEMENT ROCKS, ATHABASCA BASIN

| Sample No. | Mineral | $SiO_2$ | $ThO_2$ | $Al_2O_3$ | $Y_2O_5$ | $Ce_2O_3$ | $Dy_2O_3$ | $U_3O_8$ | $P_2O_5$ | CaO | $SrO_2$ | PbO | F | Cl | $ZrO_2$ | Totals |
|---|---|---|---|---|---|---|---|---|---|---|---|---|---|---|---|---|
| Unmineralized sandstone: | | | | | | | | | | | | | | | | |
| Mc 204-154 | de F-apatite | 0.30 | 0.04 | 0.01 | 0 | 0.06 | 0.06 | 0.03 | 38.92 | 55.45 | 0 | 0 | 4.74 | 0 | 0.02 | 97.64* |
| RL1-1192 | de F-apatite | 3.18 | 0.35 | 0.12 | 0 | 2.82 | 0.15 | 0.03 | 37.47 | 50.04 | 0 | 0.02 | 4.92 | 0.01 | 0 | 97.04* |
| Mc 204-154 | di cran gp mi | 0.57 | 1.68 | 26.93 | 0 | 7.67 | 0 | 0.04 | 22.41 | 2.93 | 5.46 | 0.82 | 0.55 | 0.23 | 0 | 69.29 |
| RL1-1192 | di cran gp mi | 0.68 | 1.59 | 26.82 | 0 | 7.29 | 0.05 | 0.01 | 23.30 | 3.17 | 6.05 | 0.73 | 0.48 | 0.18 | 0.06 | 70.40 |
| C2-120 | di cran gp mi | 1.45 | 0.33 | 30.98 | 0 | 5.39 | 0.02 | 0.02 | 25.41 | 2.03 | 9.33 | 0.05 | 0 | 0.05 | 0 | 75.07 |
| Alteration halo associated with uranium minerals: | | | | | | | | | | | | | | | | |
| Mc 204-496 | hy cran gp mi | 0.54 | 0.05 | 28.15 | 0.58 | 0.47 | 0.21 | 1.39 | 27.81 | 2.56 | 8.38 | 5.16 | 1.38 | 0.02 | 0 | 76.69 |
| Mc 204-526 | hy cran gp mi | 0.45 | 0.23 | 31.07 | 0.29 | 7.03 | 0 | 0.45 | 26.78 | 1.70 | 8.00 | 0.10 | 0.91 | 0.17 | 0 | 77.17 |
| Basement rocks: | | | | | | | | | | | | | | | | |
| Mc 178-578 | hy F-apatite | 0 | 0.02 | 0 | 0 | 0.03 | 0.09 | 0 | 42.16 | 55.35 | 0 | 0.03 | 3.75 | 0.03 | 0 | 99.89* |
| Mc 204-635 | hy F-apatite | 0 | 0 | 0.03 | 0 | 0 | 0.09 | 0 | 42.01 | 54.72 | 0.02 | 0.09 | 3.77 | 0.07 | 0 | 99.20* |
| Mc 204-676 | hy F-apatite | 0 | 0.02 | 0.04 | 0 | 0.13 | 0.08 | 0 | 43.11 | 55.19 | 0.03 | 0 | 4.04 | 0.04 | 0 | 100.98* |
| Mc 178-563 | hy cran gp mi | 23.13 | 2.00 | 22.42 | 0 | 5.45 | 0 | 0.03 | 21.64 | 2.29 | 5.73 | 0.03 | 0.75 | 0.16 | 0 | 83.64 |
| Mc 204-676 | hy cran gp mi | 0.25 | 1.25 | 29.37 | 0 | 6.51 | 0.08 | 0.05 | 26.49 | 2.34 | 6.93 | 0 | 0.95 | 0.10 | 0 | 74.33 |
| Mc 204-676 | xenotime | 0.16 | 0.32 | 0.18 | 33.28 | 0.31 | 6.27 | 0.32 | 34.20 | 0.57 | 0.05 | 0.40 | 0.80 | 0.04 | 0.34 | 77.23 |

Note: all values are quoted in wt%. Abbreviations: Mc: McArthur River area, RL: Rumple Lake area, C: west-central area of basin, de: detrital, di: diagenetic, cran gp min: crandallite-group mineral, hy: hydrothermal. * Totals corrected for oxygen assigned to $F^-$ and $Cl^-$ (Deer *et al.* 1992).

unconformity-type deposits throughout the Athabasca Basin indicate three main hydrothermal events (Wilson & Kyser 1987, Kotzer & Kyser 1995). The first hydrothermal event occurred at approximately 1500 Ma and was responsible for the transportation and deposition of the majority of the uranium ore. The second hydrothermal event occurred at approximately 950 Ma; it caused alteration and remobilization of the uranium ore. The third hydrothermal event occurred at ~300 Ma; it caused the remobilization and perhaps the precipitation of new uranium ore (Cumming & Krstic 1992, Kotzer & Kyser 1995) and altered previously deposited uranium ore. The increase in Si and Ca with decreasing age of uraninite and pitchblende (Fig. 4) is evidence that alteration of uranium minerals by subsequent fluid-circulation events occurred on a microscale and that subsequent fluids contained relatively high Si and Ca contents. During each of these subsequent fluid-circulation events, previous uranium minerals may have been variably recrystallized, with incorporation of Ca and Si, or new uranium minerals precipitated, which would have high Ca and Si contents.

The major disadvantage in determining a chemical age for a mineral lies in the inherent assumption that the total Pb present in the sample is of radiogenic origin. The sample may incorporate Pb from a variety of sources, including initial Pb from the fluid that precipitated the mineral, or radiogenic Pb during subsequent alteration and recrystallization. The diffusion coefficients of Pb in uraninite are relatively high (~$10^{-6}$ to $10^{-11}$ $cm^2/s$, at 800°C; Brandt & Perminov 1968, Yershov 1974), and Pb in uraninite does not proxy for uranium in uraninite and pitchblende, but is mostly exsolved from the crystal structure, and resides in amorphous zones (Berman 1957, Yershov 1974). Uraninite and pitchblende, therefore, may lose or incorporate Pb. Stage-1 uraninite and pitchblende that have chemical U–Pb ages that are greater than the age of the Athabasca Basin (1700 Ma) also have high Pb contents (19.2 to 25.3 wt% PbO) because radiogenic Pb was probably incorporated during subsequent fluid-circulation events. The chemical heterogeneity and wide range in chemical U–Pb ages of stage-1, 2, and 3 uranium minerals most likely resulted from variable alteration of the uranium minerals by late fluids, which preferentially removed Pb from the amorphous zones, and added Si, Ca and, less commonly, Pb.

### *Pb–Pb isotope systematics*

The $^{207}Pb/^{206}Pb$ ages of uraninite and pitchblende from both simple and complex-type deposits range from 520 to 1375 Ma, with most occurring between 1151 and 1375 Ma (Table 4). These ages are comparable to U–Pb ages of 1250–1521 Ma previously reported for presumed primary uranium mineralization in the Athabasca Basin (Hoehndorf *et al.* 1985, Carl *et al.* 1988, Ruhrmann & von Pechmann 1989, Cumming & Krstic 1992, Carl *et al.* 1992, Kotzer & Kyser 1993).

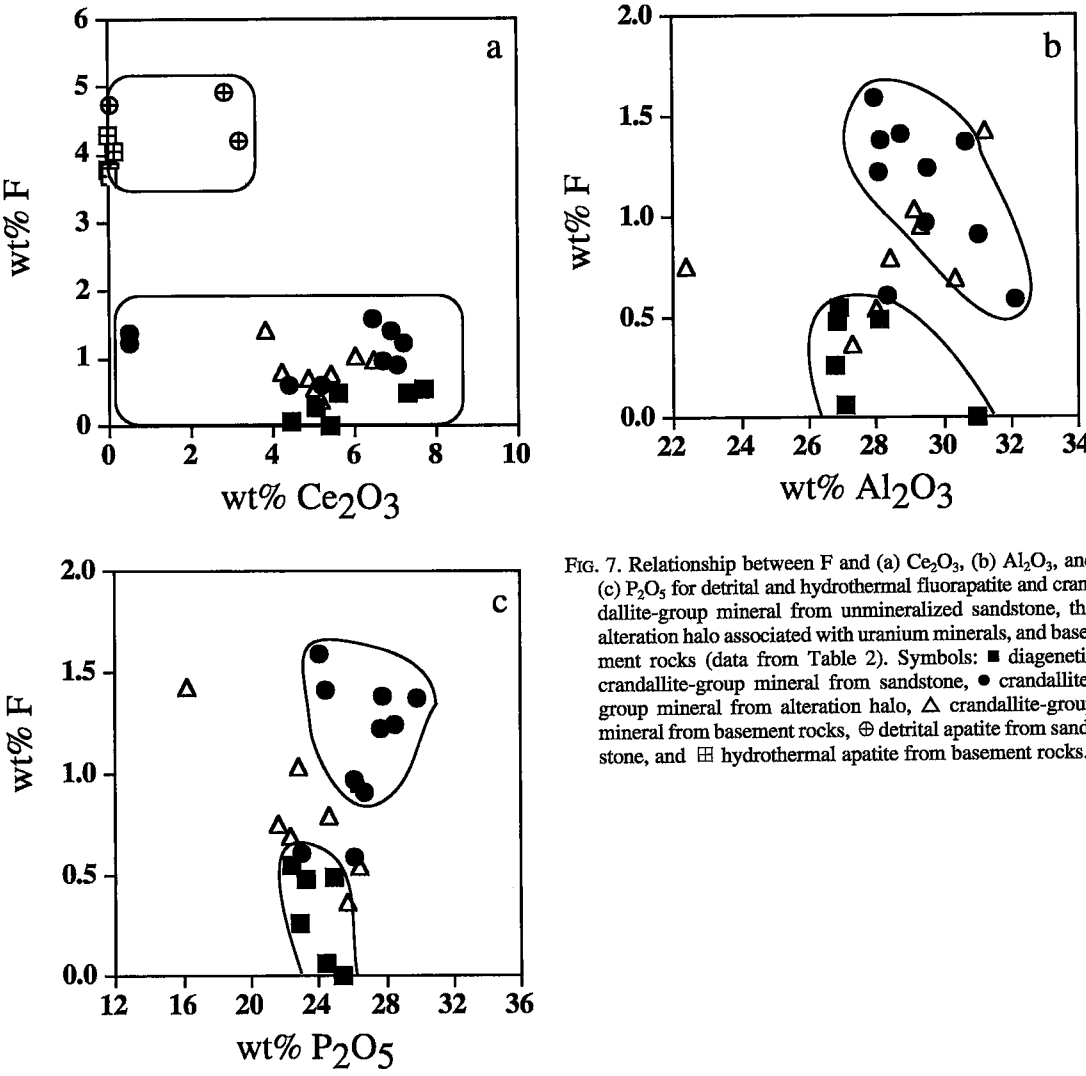


FIG. 7. Relationship between F and (a) $Ce_2O_3$, (b) $Al_2O_3$, and (c) $P_2O_5$ for detrital and hydrothermal fluorapatite and crandallite-group mineral from unmineralized sandstone, the alteration halo associated with uranium minerals, and basement rocks (data from Table 2). Symbols: ■ diagenetic crandallite-group mineral from sandstone, ● crandallite-group mineral from alteration halo, △ crandallite-group mineral from basement rocks, ⊕ detrital apatite from sandstone, and ⊞ hydrothermal apatite from basement rocks.

Calcium-rich uranium hydrate minerals and coffinite generally have younger $^{207}Pb/^{206}Pb$ ages, in the range from 194 to 1196 Ma, although most of the $^{207}Pb/^{206}Pb$ ages occur between 319 and 907 Ma (Table 4, Fig. 10a). These ages are comparable to U–Pb ages of ~200 Ma for secondary uranium minerals from Rabbit Lake (Hoeve *et al.* 1985) and elsewhere in the Athabasca Basin (Kotzer & Kyser 1993). The $^{207}Pb/^{206}Pb$ ages of uranium minerals are generally older than their chemical U–Pb ages, and therefore suggest that radiogenic lead was preferentially removed relative to uranium during the alteration of primary uranium minerals. Loss of radiogenic Pb is further substantiated by the young $^{207}Pb/^{206}Pb$ and even younger U–Pb chemical ages of Ca-rich uranium hydrate minerals and coffinite. Uranium minerals with U–Pb chemical ages that are older than the Athabasca Basin generally have high $^{204}Pb/^{206}Pb$ ratios (Table 4), which indicate that they incorporated common lead. However, occasionally, uranium minerals with U–Pb chemical ages that are older than the Athabasca Basin have low $^{204}Pb/^{206}Pb$ ratios (Table 4). This suggests that these minerals may have incorporated radiogenic lead.

*Oxygen isotope systematics*

Uranium minerals from simple and complex-type deposits from the Athabasca Basin were analyzed for their $\delta^{18}O$ values (Table 4). Stage-1 and -2 uraninite and pitchblende have $\delta^{18}O$ values that range from –32 to –19.5‰,

whereas stage-3 uraninite has $\delta^{18}O$ values between –10‰ and 0‰. "Gummite" and coffinite have $\delta^{18}O$ values that range from –15 to 0‰ (Fig. 10b). There is positive correlation between $\delta^{18}O$ values and Si and Ca contents of uraninite, pitchblende, "gummite" and coffinite (Figs. 11a,b), as is expected from the incorporation of relatively $^{18}O$-rich $SiO_2$ and CaO during formation or alteration of uranium minerals (Kotzer & Kyser 1992). Consequently, there is a negative correlation between Pb content and $\delta^{18}O$ (Fig. 11c) because the uranium minerals with the highest Si and Ca contents are the most altered and paragenetically late. However, there is little correlation between U and $\delta^{18}O$, although "gummite" and coffinite typically have lower U contents and high $\delta_{18}O$ values. Although alteration of uraninite and pitchblende has affected their oxygen isotopic and chemical compositions, and hence their mineralogy and U–Pb chemical ages, some samples of "gummite" appear to have retained a significant proportion of their original $^{207}Pb/^{206}Pb$ ratio and therefore have similar $^{207}Pb/^{206}Pb$ ages to unaltered uraninite and pitchblende (Fig. 10a).

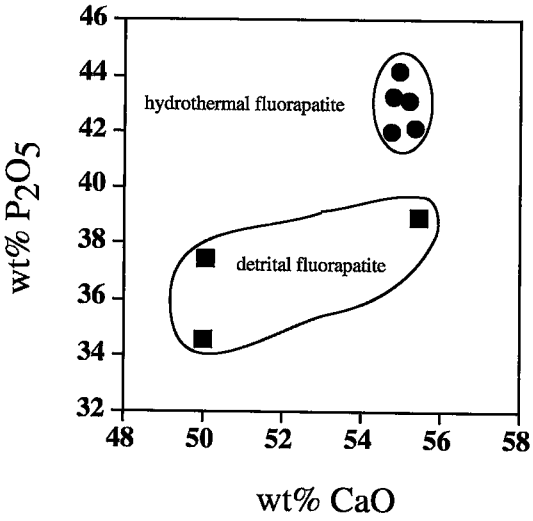


FIG. 8. Relationship between $P_2O_5$ and CaO for detrital and hydrothermal fluorapatite (data from Table 2).

The theoretical uraninite–water fractionation-factors of Hattori & Halas (1982) and Zheng (1991) indicate that the stage-1 and -2 uranium minerals would have been in equilibrium with fluids that had $\delta^{18}O$ values of less than –11‰ at *ca.* 200°C, the temperature at which the uranium deposits formed (Kotzer & Kyser 1990b). However, the dominant fluids that equilibrated with silicate and clay minerals associated with primary uranium mineralization from both simple and complex-type deposits are saline, and had $\delta^{18}O$ values of $4 \pm 2$‰ (Kotzer & Kyser 1990b, Rees 1992, Kotzer & Kyser 1993, Percival *et al.* 1993). The anomalously low $\delta^{18}O$ values of stage-1 and -2 uranium mineralization have been interpreted to result from an interaction involving uranium minerals and relatively recent, low-temperature

TABLE 3. REPRESENTATIVE RESULTS OF ELECTRON-MICROPROBE ANALYSES OF UNALTERED OR ALTERED ZIRCON FROM UNMINERALIZED SANDSTONE, ALTERATION ENVELOPE ASSOCIATED WITH URANIUM MINERALS, AND BASEMENT ROCKS, ATHABASCA BASIN

| Sample No. | Mineral | $SiO_2$ | $ThO_2$ | $Al_2O_3$ | $Y_2O_5$ | $Ce_2O_3$ | $Dy_2O_3$ | $U_3O_8$ | $P_2O_5$ | CaO | $SrO_2$ | PbO | F | Cl | $ZrO_2$ | Totals |
|---|---|---|---|---|---|---|---|---|---|---|---|---|---|---|---|---|
| Unmineralized sandstone: | | | | | | | | | | | | | | | | |
| Mc 204-154 | de zircon | 21.64 | 0.75 | 1.36 | 0 | 0.10 | 0.23 | 0.88 | 6.06 | 1.61 | 0.44 | 0.04 | 0.35 | 0.05 | 54.84 | 88.34 |
| RL1-1192 | de zircon | 34.48 | 0.06 | 0 | 0 | 0 | 0 | 0 | 0 | 0.01 | 0.49 | 0 | 0 | 0 | 62.21 | 97.65 |
| C8-242 | de zircon | 27.66 | 0 | 0.79 | 0 | 0 | 0.11 | 0.22 | 0.94 | 1.44 | 0.43 | 0 | 0.16 | 0.17 | 57.37 | 89.35 |
| Alteration halo associated with uranium minerals: | | | | | | | | | | | | | | | | |
| Mc 204-496 | unalt zircon | 35.02 | 0.27 | 0.03 | 0.43 | 0.27 | 0.16 | 0.01 | 0.20 | 0.01 | 0.69 | 0 | 0.27 | 0 | 62.82 | 100.20 |
| Mc 204-526 | unalt zircon | 34.33 | 0.23 | 0.06 | 0.46 | 0.12 | 0.18 | 0.06 | 0.07 | 0.01 | 0.71 | 0.11 | 0.18 | 0.01 | 63.88 | 100.42 |
| Mc 204-496 | alt zircon | 18.42 | 0.19 | 1.94 | 2.99 | 0.03 | 0.56 | 0.79 | 8.34 | 1.56 | 0.55 | 0.06 | 1.13 | 0.13 | 52.86 | 89.56 |
| Mc 204-526 | alt zircon | 16.84 | 0.42 | 1.82 | 4.66 | 0.20 | 0.90 | 3.66 | 10.67 | 2.45 | 0.51 | 0.08 | 3.62 | 0.12 | 45.25 | 91.18 |
| Basement rocks: | | | | | | | | | | | | | | | | |
| Mc 178-563 | unalt zircon | 33.47 | 0.11 | 0.05 | 0 | 0.16 | 0.13 | 0.25 | 0 | 0.02 | 0.78 | 0.04 | 0.27 | 0.02 | 62.09 | 97.38 |
| Mc 204-635 | unalt zircon | 32.40 | 0.27 | 0.07 | 0 | 0.32 | 0.21 | 0.14 | 0.28 | 0.29 | 0.69 | 0.13 | 0.32 | 0.12 | 59.80 | 95.04 |
| Mc 204-676 | unalt zircon | 29.30 | 0.22 | 0.20 | 0 | 0.35 | 0.24 | 0.11 | 0.38 | 0.11 | 0.73 | 0 | 0.53 | 0.03 | 61.25 | 93.44 |
| Mc 204-563 | alt zircon | 21.14 | 0.55 | 1.11 | 0 | 0.25 | 0.34 | 0.18 | 3.23 | 3.02 | 0.55 | 0.06 | 0.33 | 0.05 | 53.41 | 84.22 |
| Mc 204-635 | alt zircon | 23.56 | 0.32 | 0.92 | 0 | 0.25 | 0.45 | 0.47 | 2.25 | 2.07 | 0.57 | 0.01 | 0.51 | 0.09 | 52.81 | 84.30 |

Note: all values are quoted in wt%. Abbreviations: Mc: McArthur River area, RL: Rumple Lake area, C: west-central area of basin, de: detrital, unalt: unaltered, alt: altered.

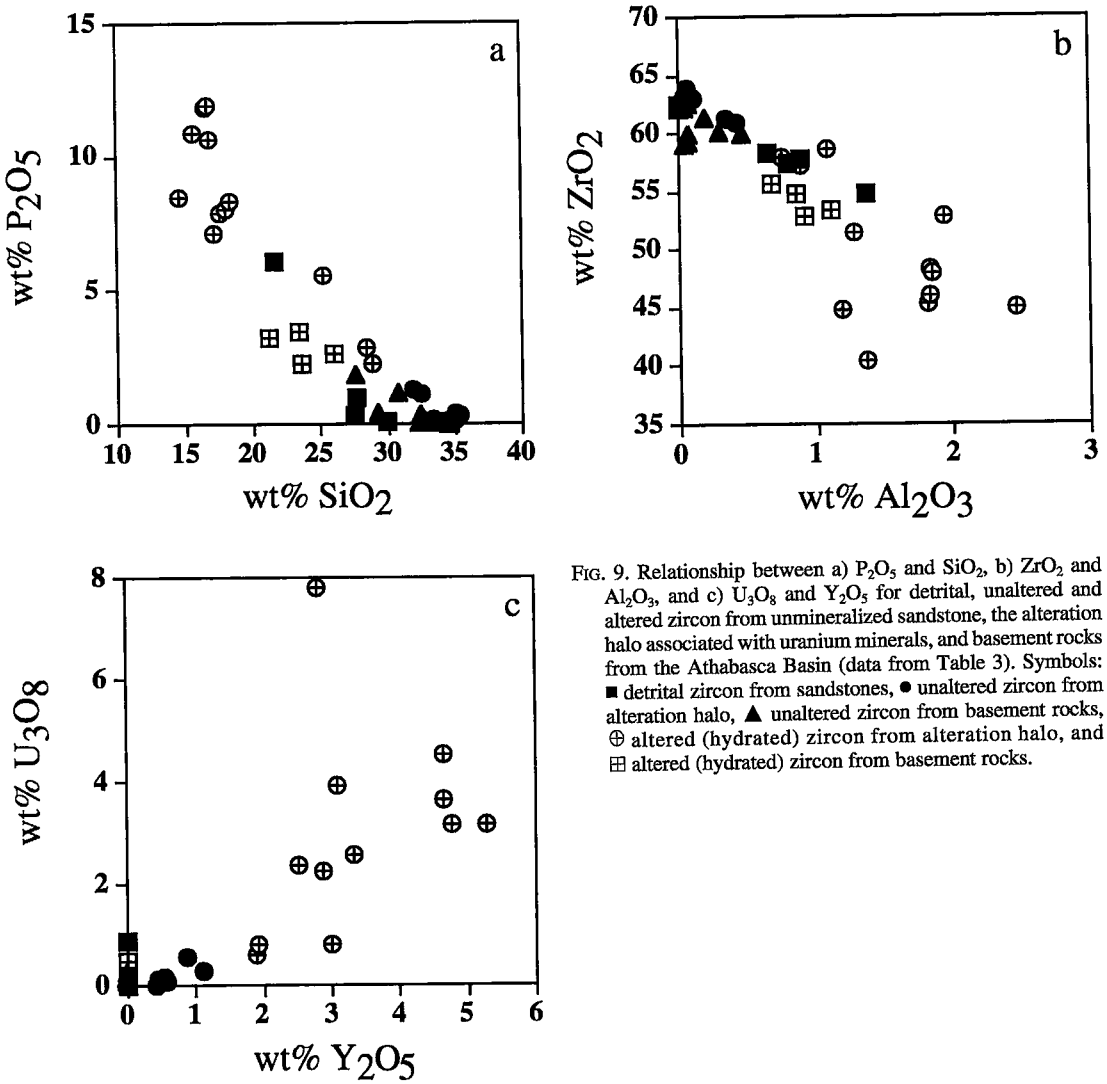


FIG. 9. Relationship between a) $P_2O_5$ and $SiO_2$, b) $ZrO_2$ and $Al_2O_3$, and c) $U_3O_8$ and $Y_2O_5$ for detrital, unaltered and altered zircon from unmineralized sandstone, the alteration halo associated with uranium minerals, and basement rocks from the Athabasca Basin (data from Table 3). Symbols: ■ detrital zircon from sandstones, ● unaltered zircon from alteration halo, ▲ unaltered zircon from basement rocks, ⊕ altered (hydrated) zircon from alteration halo, and ⊞ altered (hydrated) zircon from basement rocks.

meteoric fluids with $\delta^{18}O$ values of *ca.* –18‰ (Hoekstra & Katz 1955, Hattori *et al.* 1978, Kotzer & Kyser 1990b, 1993). If confirmed, the high reflectivities and lack of alteration (*i.e.*, low Si and Ca) of stage-1 and -2 uranium minerals would require that uranium minerals can exchange oxygen isotopes with a fluid with negligible modification of their chemical compositions and textures. However, results of Kotzer & Kyser (1993) and this study show that a positive correlation exists between $\delta^{18}O$ values and the Si and Ca contents of the minerals (Fig. 11), even for relatively unaltered uraninite and pitchblende samples, and that uranium minerals in the deposits altered to "gummite" and coffinite as a result of interaction with fluids. Therefore, the most pristine uranium minerals, which have the lowest $\delta^{18}O$ values, do not have the prerequisite chemical or mineralogical compositions to be indicative of interaction with late fluids.

The theoretical fractionation-factors of Hattori & Halas (1982) and Zheng (1991), used by Kotzer & Kyser (1990b, 1993), require several assumptions concerning errors on force constants and an estimate of frequency shifts, which create significant uncertainties for the vibrational frequencies used in calculating reduced partition-coefficients (O'Neil 1986). In addition, theoretical uraninite–water fractionation-factors rely on

TABLE 4. SAMPLE DESCRIPTION, Pb ISOTOPE AND $^{87}Sr/^{86}Sr$ RATIOS, OXYGEN ISOTOPIC COMPOSITION, AND U–Pb CHEMICAL AGES OF URANIUM MINERALS FROM THE ATHABASCA BASIN

| Sample No. DDH/depth | Remarks | $^{204}Pb/^{206}Pb$ | $^{207}Pb/^{206}Pb$ | $^{87}Sr/^{86}Sr$ | $\delta^{18}O$ (‰) | U-Pb chemical Age (Ma) | $^{207}Pb/^{206}Pb$ Ages (Ma) | |
|---|---|---|---|---|---|---|---|---|
| McArthur R.: | | | | | | | | |
| 204-503 | stage-1 uran | 0.000035 (37) | 0.081144 (48) | 0.71383 (5) | -26.5 | 1334 | 1225±1 | |
| 204-503 | Ca-U hydrate | 0.000021 (3) | 0.079949 (12) | 0.71467 (2) | -4.6 | 842 | 1196±0.3 | |
| 230-528 | stage-1 uran | 0.000005 (1) | 0.080124 (7) | 0.71471 (2) | **-12.3 | 1230 | 1200±0.2 | |
| 236-515 | stage-2 uran | 0.000010 (1) | 0.065810 (3) | 0.71485 (7) | -19.5 | 723 | 800±0.1 | |
| 236-515 | Ca-U hydrate | 0.000038 (15) | 0.065337 (16) | 0.71490 (4) | 2.7 | 69 | 785±0.5 | |
| 236-511 | stage-2 uran | 0.000035 (3) | 0.071249 (11) | 0.71390 (1) | -28.0 | 1142 | 965±0.3 | |
| 236-511 | stage-3 uran | 0.000014 (17) | 0.074572 (22) | 0.71405 (4) | **-10.4 | 358 | 1057±0.6 | |
| Cigar L.: | | | | | | | | |
| 480-176 | stage-3 uran | 0.001028 (1) | 0.093299 (3) | 0.70974 (3) | -9.2 | 398 | 1494±0.1 | (*1166) |
| Key L.: | | | | | | | | |
| 470-6 | Ca-U hydrate | 0.000029 (3) | 0.061097 (4) | 0.71046 (7) | 2.5 | 103 | 643±0.2 | |
| 470-10-7 | stage-2 uran | 0.000552 (11) | 0.086383 (11) | 0.70900(123) | **-10.4 | 507 | 1347±0.3 | (*1163) |
| 470-10-7 | Ca-U hydrate | 0.000313 (1) | 0.085998 (4) | 0.71001 (3) | -1.2 | 285 | 1338±0.1 | (*1236) |
| 478-14 | stage-1 uran | 0.000083 (2) | 0.080766 (6) | 0.71396 (7) | -22.7 | 1666 | 1315±0.1 | (*1187) |
| 478-14 | Ca-U hydrate | 0.000777 (2) | 0.080425 (10) | 0.71014 (3) | -0.3 | 549 | 1207±0.3 | (*907) |
| Sue Zone: | | | | | | | | |
| 211-136 | stage-3 uran | 0.000022 (1) | 0.049975 (3) | 0.71002 (1) | -1.4 | 135 | 194±0.1 | |
| 247 | stage-2 uran | 0.000126 (1) | 0.059462 (3) | 0.70960 (3) | -20.8 | 1420 | 584±0.2 | (*516) |
| 528-95 | stage-1pitch | 0.000013 (2) | 0.078172 (6) | 0.70935 (3) | -25.0 | 1305 | 1151±0.1 | |
| 528-129 | stage-1 uran | 0.000231 (1) | 0.089115 (11) | 0.70912 (13) | -28.0 | 1599 | 1407±0.3 | (*1335) |
| 528-129 | stage-1 uran | 0.000079 (2) | 0.087347 (13) | 0.70889 (2) | **-12.0 | 1403 | 1368±0.3 | (*1344) |
| 528-129 | stage-1 uran | 0.000068 (2) | 0.088610 (20) | 0.70692 (1) | -32.0 | 1649 | 1396±0.4 | (*1375) |
| 528-129 | stage-1 uran | 0.000521 (62) | 0.089697 (75) | 0.70964 (1) | n.a. | n.a. | 1419±2 | (*1254) |
| Eagle Pt. North: | | | | | | | | |
| 277-49 | Ca-U hydrate | 0.000004 (1) | 0.060701 (2) | 0.71119 (1) | -16.0 | 409 | 629±0.2 | |
| 779-57 | stage-2 uran | n.a. | 0.062322 (6) | 0.71269 (3) | -24.0 | 810 | 685±0.2 | |
| 779-57 | stage-2 uran | n.a. | n.a. | n.a. | -20.0 | 829 | n.a. | |
| 779-57 | stage-2 uran | 0.000004 (1) | 0.063131 (3) | 0.71332 (20) | -24.0 | 938 | 713±0.1 | |
| 779-57 | stage-3 uran | 0.000016 (8) | 0.063821 (15) | 0.71415 (86) | -14.0 | 596 | 736±0.5 | |
| Eagle Pt. South: | | | | | | | | |
| 213-213 | coffinite | 0.000028 (4) | 0.064692 (11) | 0.71511 (2) | -0.6 | 211 | 764±0.4 | |
| 213-221 | stage-3 uran | 0.000021 (1) | 0.057743 (4) | 0.70910 (2) | -10.4 | n.a. | 520±0.2 | |
| 23-224 | coffinite | n.a. | 0.062533 (3) | 0.70990 (26) | -15.7 | 284 | 692±0.1 | |
| Ep2 | stage-2 uran | n.a. | 0.064159 (38) | 0.71447 (14) | -18.7 | n.a. | 747±0.1 | |

Note: numbers in parentheses indicate errors (2σ). All analyses are unspiked. * $^{207}Pb/^{206}Pb$ ages corrected for common Pb. ** Samples containing quartz that could not be removed. Abbreviations: n.a.: not detected or not measured, L.: Lake, R.: River, Pt.: Point, uran: uraninite, pitch: pitchblende, DDH: diamond drill hole. Depth is reported in meters.

pure end-member structures to simplify the calculations, because it is difficult to adequately estimate frequency shifts caused by isotopic substitution in more complex structures. However, natural uraninite and pitchblende in the Athabasca Basin are complex minerals that consist of both $U^{6+}$and $U^{4+}$ in addition to trace amounts of Ca, Si, *REE* and Th (Berman 1957, Powers & Stauffer 1985, Kotzer & Kyser 1993, Fayek & Kyser 1993). The theoretical fractionation-factors of Hattori & Halas (1982) and Zheng (1991), therefore, may be unreliable for most samples of uraninite and pitchblende because the structure of end-member uraninite does not adequately represent natural samples. The pristine mineralogy and simple chemistry of stage-1 and -2 uraninite indicate that they have retained much of their original oxygen isotopic composition, so that the theoretical fractionation-factors for uraninite–water are not appropriate for these systems. Given that the uraninite formed at 200°C from waters with a $\delta^{18}O$ value of *ca.* 4‰ and using the theoretical fractionation-factors, the calculated $\delta^{18}O$ values of uraninite and pitchblende would be expected to range

FIG. 10. Relationship between $\delta^{18}O$ values and (a) $^{207}Pb/^{206}Pb$ ages, and (b) U–Pb chemical ages for uranium minerals from the Athabasca Basin (data from Tables 1 and 4). The "gummite" and coffinite have significantly different $\delta^{18}O$ values relative to uraninite and pitchblende from which they formed, yet have partially retained their original $^{207}Pb/^{206}Pb$ ages. Symbols: ■ uraninite, ○ "gummite", and △ coffinite.

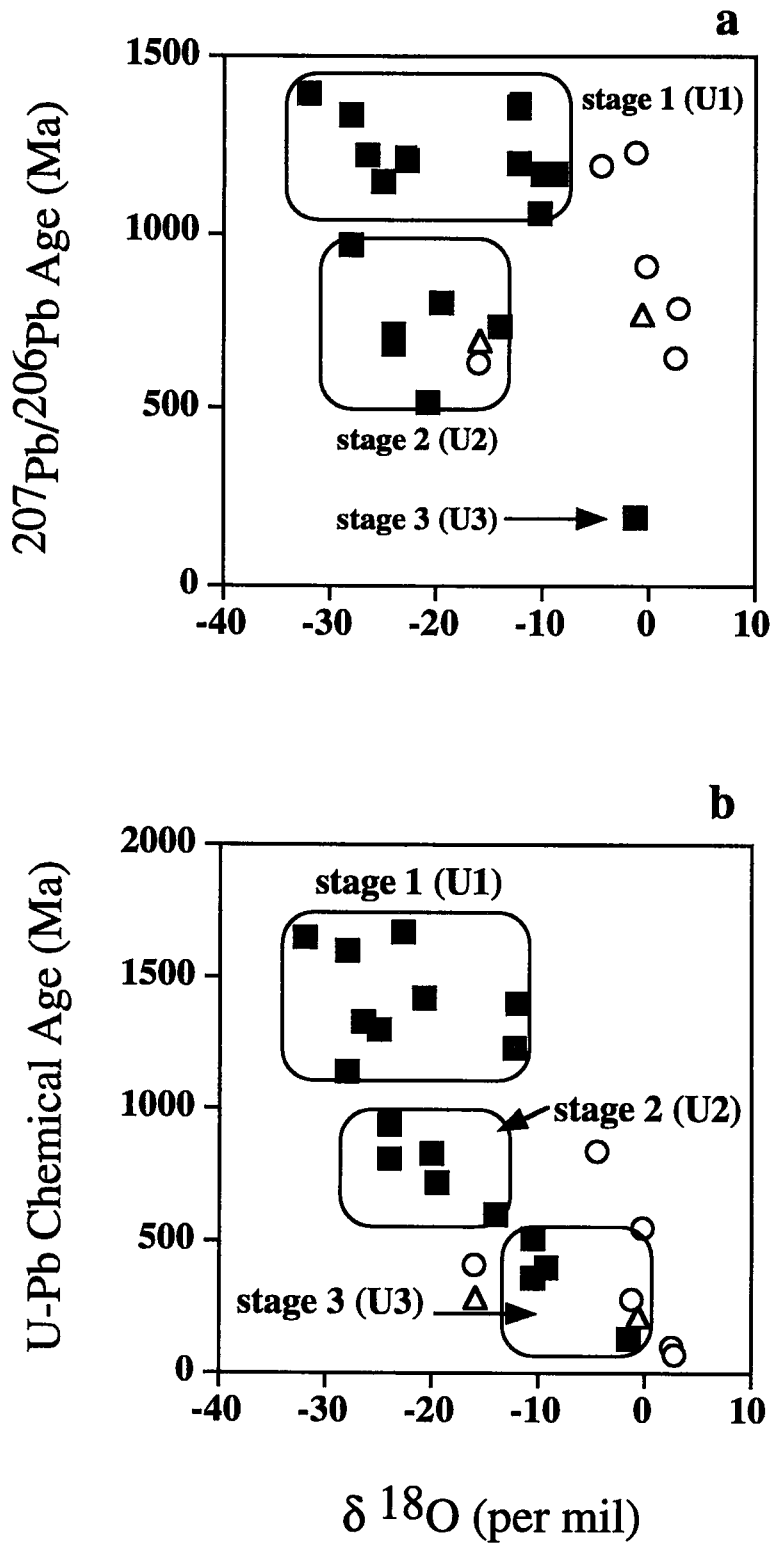
a
1500
1000
500
0
$^{207}Pb/^{206}Pb$ Age (Ma)
stage 1 (U1)
stage 2 (U2)
stage 3 (U3)
-40
-30
-20
-10
0
10
b
2000
1500
1000
500
0
U-Pb Chemical Age (Ma)
stage 1 (U1)
stage 2 (U2)
stage 3 (U3)
-40
-30
-20
-10
0
10
$\delta^{18}O$ (per mil)

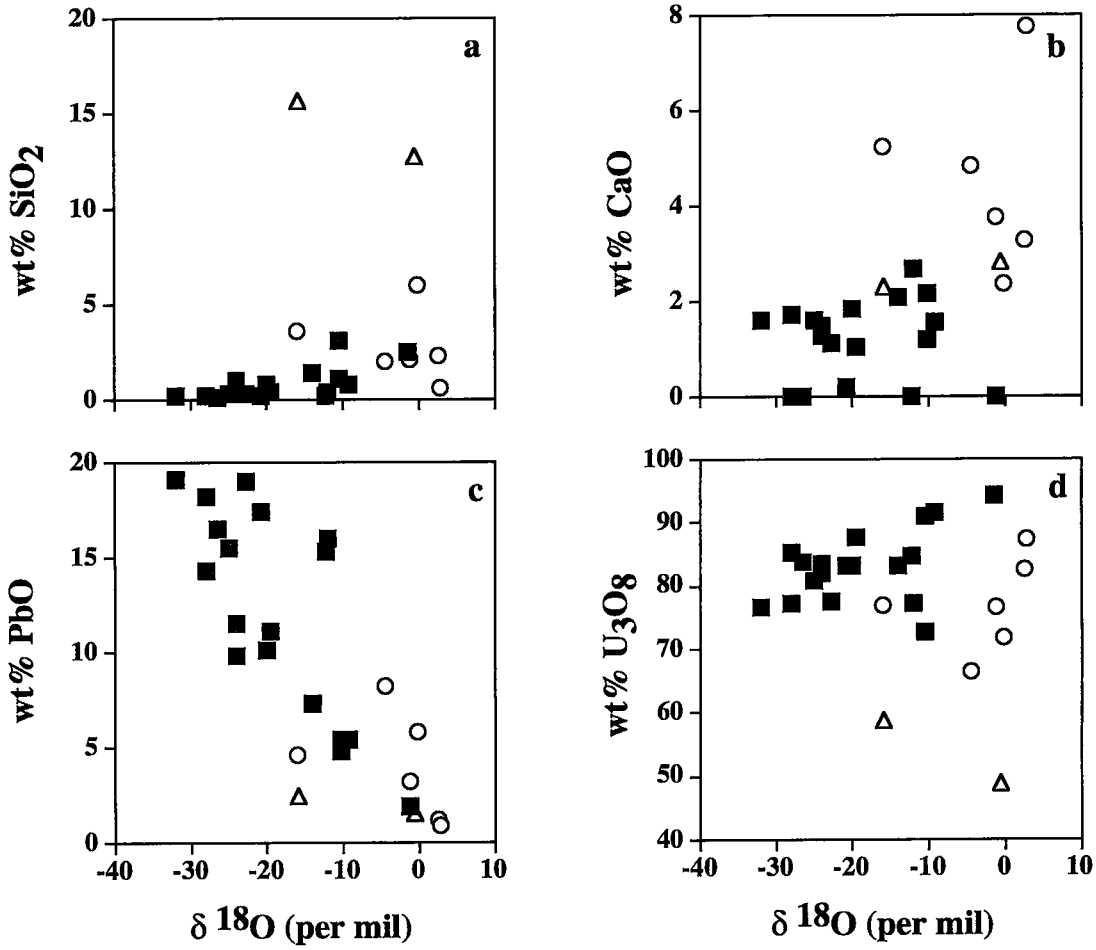


FIG. 11. Relationship between $\delta^{18}O$ values and (a) $SiO_2$, (b) CaO, (c) PbO, and d) $U_3O_8$ contents of uranium minerals from the Athabasca Basin (data from Tables 1 and 4). Symbols: ■ uraninite, ○ "gummite", and △ coffinite.

between –5 and –10‰. Therefore, an interaction between late meteoric water and uranium minerals from the deposits has partially affected the chemistry and oxygen isotopic composition, and significantly affected the Pb content of uraninite and pitchblende.

*Sr isotope systematics*

Illite replacing feldspar in metasedimentary rocks of the basement has high $^{87}Sr/^{86}Sr$ ratios (0.76970 to 2.96382) relative to illite from diagenetically altered Athabasca Group sandstones, which has $^{87}Sr/^{86}Sr$ ratios that range from 0.70626 to 0.71132 (Pagel *et al.* 1993, Kotzer & Kyser 1995). Therefore, fluids originating from the basement rocks may have had appreciably higher $^{87}Sr/^{86}Sr$ ratios than fluids in the basin. Consequently, the hydrothermal clay and silicate minerals that formed as a result of mixing between these distinct fluids should have $^{87}Sr/^{86}Sr$ ratios proportional to the amount of basin and basement fluids (Fig. 12a). As such, uraninite formed as a result of mixing between basin and basement fluids also should have $^{87}Sr/^{86}Sr$ ratios proportional to the amount of basin and basement fluids.

Uranium minerals from simple-type deposits, hosted entirely by basement rocks, have $^{87}Sr/^{86}Sr$ ratios ranging from 0.70692 to 0.71002 (Table 4, Fig. 12b), whereas uranium minerals from complex-type deposits, which formed at the unconformity and are hosted partially by sandstone, have $^{87}Sr/^{86}Sr$ ratios ranging from 0.71269 to 0.71490 (Table 4, Fig. 12b). The high $^{87}Sr/^{86}Sr$ ratios

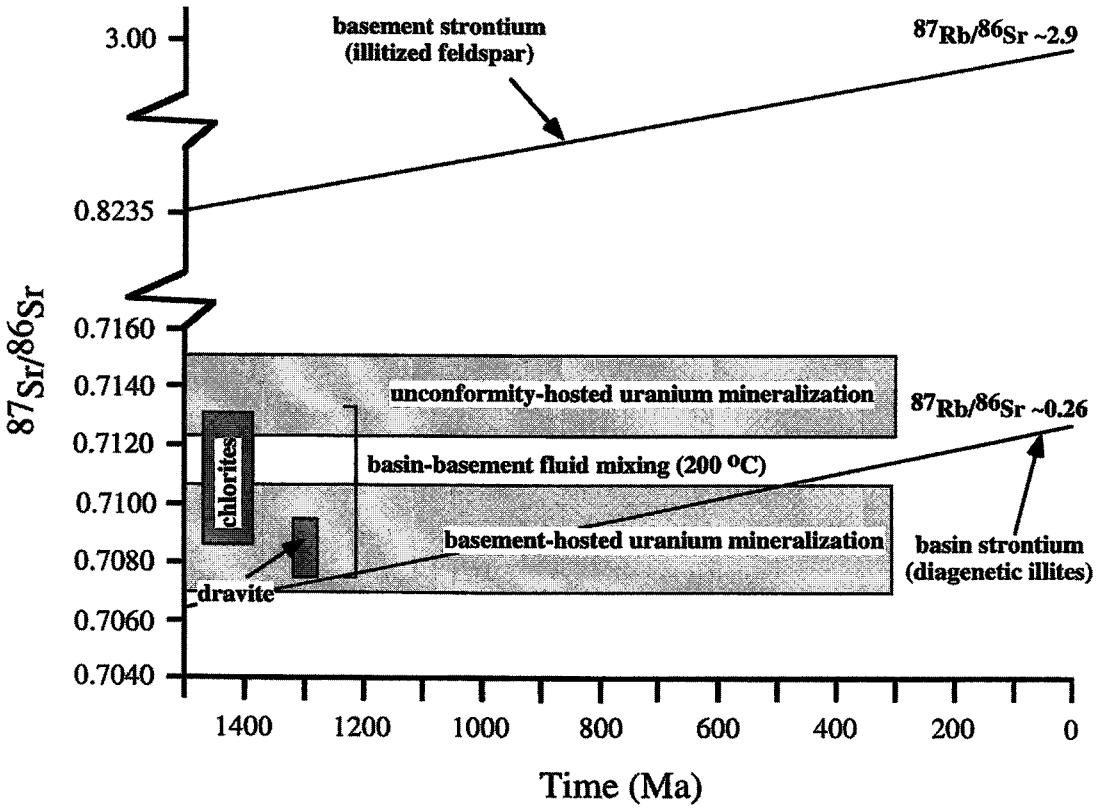


FIG. 12a. Evolution of strontium in the Athabasca Basin, showing measured $^{87}Rb/^{86}Sr$ and $^{87}Sr/^{86}Sr$ ratios for illite from altered basement rocks (basement strontium) and from diagenetic illite in sandstones (basin strontium). Also shown is the range $^{87}Sr/^{86}Sr$ ratios of dravite and chlorite, which formed from variable mixing between basement- and basin-derived fluids, and the relatively restricted range in $^{87}Sr/^{86}Sr$ ratios of sandstone-unconformity-hosted (complex-type) and basement-hosted (simple-type) uranium minerals (modified from Kotzer & Kyser 1995).

of uranium minerals from complex-type deposits and the high concentration of associated sulfides indicate that appreciable quantities of basement fluid were involved in the formation of these deposits. Uranium minerals and sulfides most likely precipitated when the oxidizing, uranium-rich basinal brine mixed with the sulfide-rich, reducing basement fluid. Conversely, the low $^{87}Sr/^{86}Sr$ ratios of basement-hosted uranium mineralization in simple-type deposits, and the lack of associated sulfides, reflect a high proportion of basin fluid involved in the formation of these deposits. The precipitation of uranium minerals most likely resulted from the interaction between the oxidizing, uranium-rich basinal brine and the reducing basement rocks, rather than mixing with a basement-derived fluid.

Some unconformity-type uranium deposits (Eagle Point and Key Lake) contain uraninite and pitchblende with variable $^{87}Sr/^{86}Sr$ ratios (Table 4). Uranium minerals with low $^{87}Sr/^{86}Sr$ ratios generally have younger $^{207}Pb/^{206}Pb$ and chemical U–Pb ages (1000 to 300 Ma) relative to uranium minerals from the same deposit with high $^{87}Sr/^{86}Sr$ ratios, which have $^{207}Pb/^{206}Pb$ and chemical U–Pb ages near 1500 Ma. These results imply that involvement of basement fluid in the formation of the uranium deposits was mainly restricted to the earliest hydrothermal events. Subsequent fluid-flow events involved basin fluids with a minimal contribution from basement-derived fluids.

Calcium-rich uranium hydrate minerals and coffinite have $^{87}Sr/^{86}Sr$ ratios that are similar to those of uraninite and pitchblende from which they formed (Fig. 12b). Therefore, subsequent alteration of uraninite and pitchblende during late fluid-flow events did not substantially affect their initial $^{87}Sr/^{86}Sr$ ratio.

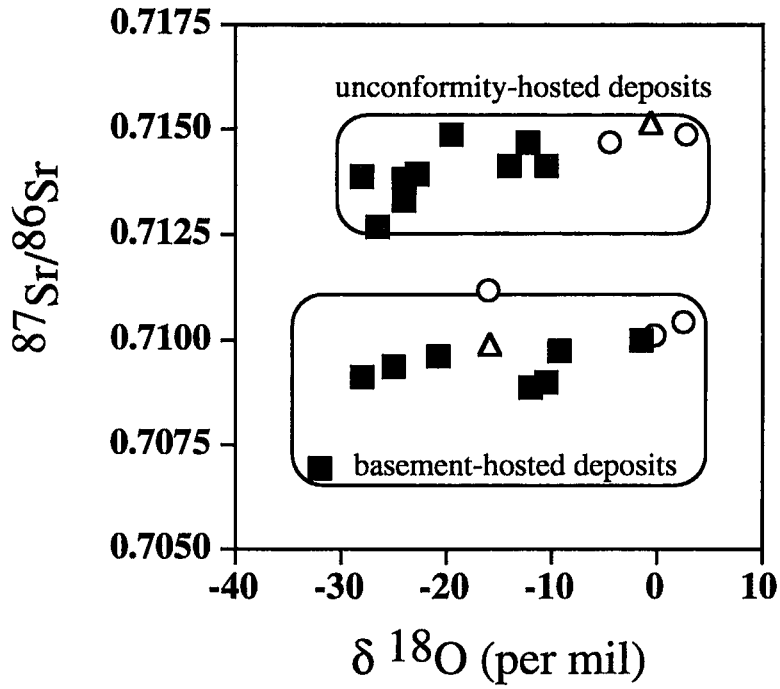


FIG. 12b. Relationship between $^{87}Sr/^{86}Sr$ and $\delta^{18}O$ values of uranium minerals from the unconformity-hosted (complex-type) and basement-hosted (simple-type) uranium deposits (data from Table 4). Symbols: ■ uraninite–pitchblende, ○ "gummite", and △ coffinite.

## RARE-EARTH-ELEMENT GEOCHEMISTRY

### *Unmineralized sandstone, clay alteration associated with uranium mineralization, and basement rocks*

Samples of unmineralized sandstone from several formations from the Athabasca Basin have low total *REE* (~100 ppm) and *LREE*-enriched normalized patterns, with a negative Eu anomaly (Table 5, Fig. 13). The minerals that most likely contribute to the *REE* pattern of the sandstone are the early diagenetic crandallite-group and clay minerals and detrital fluorapatite, which have similar *REE* patterns to the whole-rock sandstone samples (Quirt *et al.* 1991). Detrital zircon, which is relatively enriched in the *HREE* (Grauch 1989), appears to have little effect on the normalized *REE* patterns of the sandstone, because most of it has been removed during diagenesis.

Alteration halos associated with uranium mineralization have similar *LREE*-enriched normalized *REE* patterns, but generally higher total *REE* contents (~1200 ppm, Fig. 13). The higher concentration of total *REE* in the alteration halos is due to the increased concentration of clay minerals, tourmaline, and the crandallite-group minerals (*LREE*-enriched phosphate minerals), which are more abundant than in normal Athabasca Group sandstones. Zircon and xenotime (*HREE* phosphate) have little effect on the normalized *REE* pattern of samples from the alteration halo because they are not present in significant proportions. Relatively unaltered basement rocks have flatter normalized *REE* patterns relative to unmineralized sandstone with higher *HREE* contents (Table 5, Fig. 13). The relatively high concentrations of the *HREE* associated with these rocks are most likely due to the presence of significant quantities of garnet and zircon, which typically capture the *HREE* (Grauch 1989, McLennan 1989, Fleet & Pan 1995).

### *Uranium mineralization*

*REE* contents of uraninite, pitchblende, "gummite" and coffinite from five deposits (sandstone- and basement-hosted) are as high as 12,000 ppm (Table 6). Uraninite, pitchblende, "gummite" and coffinite are *HREE*-enriched and have similar normalized *REE* patterns (Fig. 14). However, "gummite" minerals and coffinite have slightly lower total *REE* contents, indicating that the

TABLE 5. REE CONCENTRATIONS OF REPRESENTATIVE SAMPLES OF BARREN SANDSTONE, CLAY ALTERATION ASSOCIATED WITH URANIUM MINERALS, AND BASEMENT ROCKS FROM THE ATHABASCA BASIN

| | McArthur River Area (DDH-204) | | | | | | Rumple Lake (East-Central Basin) (DDH-1) | | | | | | West-Central Basin (DDH-CSP8) | | | | | Maybell River (Western Basin) (DDH-84) | | | | | |
|---|---|---|---|---|---|---|---|---|---|---|---|---|---|---|---|---|---|---|---|---|---|---|---|
| Depth (m) | 154 | 465 | 491 | 500 | 663 | 676 | 730 | 949 | 1192 | 1236 | 1402 | 1544 | 225 | 302 | 377 | 422 | 496 | 43 | 187 | 296 | 326 | 339 | |
| Element | sand. | sand. | sand. | alt. | bsmt. | bsmt. | sand. | sand. | sand. | sand. | sand. | bsmt. | sand. | sand. | sand. | sand. | sand. | sand. | sand. | sand. | sand. | bsmt. | Chondrite* |
| Th | 4.1 | 3.2 | 3.4 | 28.6 | 49.3 | 14.9 | 1.9 | 2.3 | 2.4 | 4.2 | 5.3 | 1.9 | 1.8 | 2.4 | 5.5 | 4.8 | 14.5 | 2.5 | 3.1 | 7.9 | 30.8 | 0.98 | - |
| U | 2.7 | 7.1 | 3.2 | 1072 | 6.2 | 3.7 | 0.32 | 0.35 | 0.58 | 0.40 | 0.63 | 3.7 | 0.46 | 0.59 | 0.98 | 0.62 | 1.6 | 0.54 | 0.64 | 0.41 | 1.4 | 2.3 | - |
| Th/U | 1.5 | 0.45 | 1.1 | 0.03 | 7.9 | 4.0 | 6.1 | 6.6 | 5.8 | 10.5 | 8.4 | 0.51 | 3.9 | 4.0 | 5.6 | 7.8 | 9.2 | 4.6 | 4.9 | 19.3 | 22.0 | 0.42 | - |
| La | 10.9 | 9.7 | 4.3 | 244 | 49.4 | 38.3 | 9.0 | 8.7 | 7.0 | 7.5 | 10.4 | 3.1 | 10.5 | 19.5 | 28.6 | 27.0 | 47.6 | 7.6 | 10.5 | 15.4 | 33.1 | 10.2 | 0.376 |
| Ce | 23.7 | 18.7 | 7.6 | 450 | 96.2 | 73.0 | 16.9 | 18.0 | 14.9 | 17.1 | 24.0 | 6.5 | 21.5 | 43.3 | 49.1 | 53.9 | 74.1 | 15.2 | 21.9 | 28.9 | 63.3 | 10.8 | 0.957 |
| Pr | 2.3 | 2.2 | 0.79 | 55.7 | 11.4 | 8.5 | 1.8 | 1.9 | 1.6 | 1.8 | 2.7 | 0.87 | 2.4 | 4.6 | 6.1 | 6.4 | 10.9 | 1.7 | 2.4 | 3.3 | 7.5 | 2.6 | 0.137 |
| Nd | 7.9 | 7.8 | 2.7 | 230 | 40.2 | 30.7 | 5.4 | 6.1 | 5.4 | 5.9 | 10.2 | 3.8 | 8.6 | 16.5 | 19.7 | 21.8 | 38.1 | 5.7 | 8.6 | 11.4 | 24.6 | 9.8 | 0.711 |
| Sm | 1.2 | 1.4 | 0.46 | 42.3 | 6.5 | 5.0 | 0.66 | 0.90 | 0.90 | 0.89 | 1.8 | 0.93 | 1.6 | 3.0 | 3.1 | 3.4 | 6.4 | 0.97 | 1.4 | 2.0 | 4.0 | 2.3 | 0.231 |
| Eu | 0.21 | 0.24 | 0.09 | 9.7 | 0.88 | 0.85 | 0.09 | 0.14 | 0.12 | 0.13 | 0.19 | 0.25 | 0.30 | 0.54 | 0.54 | 0.51 | 1.0 | 0.15 | 0.26 | 0.41 | 0.58 | 0.67 | 0.087 |
| Gd | 0.91 | 1.3 | 0.43 | 72.5 | 4.6 | 5.1 | 0.54 | 0.72 | 0.70 | 0.65 | 1.1 | 1.3 | 1.5 | 2.5 | 2.7 | 2.1 | 5.7 | 0.81 | 1.4 | 1.7 | 3.4 | 3.6 | 0.306 |
| Tb | 0.12 | 0.17 | 0.06 | 9.1 | 0.57 | 0.93 | 0.06 | 0.08 | 0.08 | 0.06 | 0.09 | 0.23 | 0.21 | 0.28 | 0.38 | 0.36 | 0.66 | 0.12 | 0.24 | 0.17 | 0.38 | 0.89 | 0.058 |
| Dy | 0.53 | 0.90 | 0.40 | 39.3 | 2.9 | 6.5 | 0.29 | 0.45 | 0.34 | 0.33 | 0.35 | 1.4 | 1.1 | 1.3 | 2.4 | 2.2 | 4.1 | 0.69 | 1.6 | 0.72 | 1.6 | 7.4 | 0.381 |
| Ho | 0.10 | 0.17 | 0.08 | 4.9 | 0.52 | 1.1 | 0.06 | 0.07 | 0.07 | 0.05 | 0.06 | 0.31 | 0.20 | 0.23 | 0.49 | 0.44 | 0.85 | 0.12 | 0.29 | 0.10 | 0.28 | 1.5 | 0.0851 |
| Er | 0.23 | 0.52 | 0.26 | 10.0 | 1.3 | 2.7 | 0.13 | 0.27 | 0.16 | 0.19 | 0.20 | 0.90 | 0.53 | 0.73 | 1.4 | 1.3 | 2.8 | 0.40 | 0.77 | 0.29 | 0.76 | 4.1 | 0.249 |
| Tm | 0.03 | 0.09 | 0.04 | 1.1 | 0.20 | 0.33 | 0.02. | 0.04 | 0.03 | 0.03 | 0.03 | 0.15 | 0.10 | 0.11 | 0.24 | 0.22 | 0.47 | 0.06 | 0.09 | 0.04 | 0.11 | 0.63 | 0.0356 |
| Yb | 0.24 | 0.60 | 0.32 | 6.0 | 1.4 | 1.9 | 0.17 | 0.24 | 0.24 | 0.24 | 0.21 | 0.88 | 0.60 | 0.70 | 1.7 | 1.5 | 3.3 | 0.39 | 0.59 | 0.30 | 0.82 | 3.9 | 0.248 |
| Lu | 0.04 | 0.11 | 0.04 | 0.86 | 0.19 | 0.27 | 0.02 | 0.05 | 0.04 | 0.04 | 0.04 | 0.15 | 0.09 | 0.1 | 0.25 | 0.19 | 0.54 | 0.07 | 0.09 | 0.05 | 0.13 | 0.59 | 0.0381 |
| Y | 2.1 | 4.8 | 2.7 | 120 | 13.6 | 29.9 | 1.3 | 1.8 | 1.9 | 1.5 | 1.6 | 9.1 | 5.3 | 6.1 | 14.0 | 12.0 | 24.5 | 3.3 | 8.4 | 2.9 | 8.5 | 42.4 | 2.25 |
| Total | 50.6 | 48.7 | 20.3 | 1296 | 230 | 205 | 36.3 | 39.4 | 33.5 | 36.4 | 52.9 | 29.9 | 54.4 | 99.6 | 131 | 133 | 221 | 37.5 | 58.4 | 67.7 | 149 | 101 | 6.14 |
| Total LREE | 46.3 | 40.0 | 16.0 | 1032 | 205 | 156 | 33.8 | 35.7 | 29.9 | 33.4 | 49.2 | 15.4 | 44.8 | 87.6 | 107 | 113 | 178 | 31.5 | 44.9 | 61.5 | 133 | 36.4 | 2.50 |
| Total HREE | 2.2 | 3.9 | 1.6 | 144 | 11.7 | 18.8 | 1.3 | 1.9 | 1.7 | 1.6 | 2.08 | 5.4 | 4.3 | 5.9 | 9.5 | 8.2 | 18.4 | 2.7 | 5.1 | 3.3 | 7.4 | 22.6 | 1.40 |
| HREE/LREE | 0.05 | 0.10 | 0.10 | 0.14 | 0.06 | 0.12 | 0.04 | 0.05 | 0.06 | 0.05 | 0.04 | 0.35 | 0.10 | 0.07 | 0.09 | 0.07 | 0.10 | 0.09 | 0.11 | 0.05 | 0.06 | 0.62 | 0.561 |
| La/Yb | 45.5 | 16.2 | 13.5 | 40.9 | 36.3 | 20.3 | 52.7 | 36.2 | 29.3 | 31.4 | 49.6 | 3.5 | 17.4 | 27.9 | 17.3 | 18.6 | 14.4 | 19.4 | 17.8 | 51.4 | 40.3 | 2.6 | 1.52 |
| La/Y | 5.2 | 2.0 | 1.6 | 2.0 | 3.6 | 1.3 | 7.2 | 4.8 | 3.7 | 5.1 | 6.4 | 0.34 | 2.0 | 3.2 | 2.0 | 2.3 | 1.9 | 2.3 | 1.2 | 5.3 | 3.9 | 0.24 | 0.17 |

Note: all values are reported in ppm
*From Taylor and McLennan (1985)
Abbreviations: sand.=sandstone; alt.=alteration; bsmt.=basement; DDH=diamond drill hole.

*REE* are not substantially remobilized or fractionated during alteration of uraninite by late meteoric waters. Similar *REE* patterns have been documented for uranium minerals in Proterozoic basins in Australia (McLennan & Taylor 1979) and other deposits from the Athabasca and Beaverlodge areas (Fryer & Taylor 1987, Quirt *et al.* 1991, Fayek & Kyser 1993).

Abundant sulfides and arsenides and high $^{87}Sr/^{86}Sr$ ratios associated with complex-type uranium deposits (Fig. 15) indicate that uranium deposition occurred under reducing conditions, where a large volume of basement-derived fluid interacted with the oxidizing basinal brine. The presence of altered garnet and zircon, and the abundance of hydrothermal fluorapatite and xenotime in basement rocks, indicate that fluid derived from basement rocks contained high concentrations of *REE* in addition to P, F and a variety of other elements (Fig. 15). Uraninite and pitchblende from these deposits have the highest *REE* contents, flatter *REE* patterns, with very high *HREE* contents. The relatively high Ce contents (Table 6) indicate that Ce was once $Ce^{4+}$, was subsequently reduced to $Ce^{3+}$, and therefore was not appreciably fractionated from the rest of the *REE* (Figs. 14a, b, c). In contrast, uraninite and pitchblende from simple-type uranium deposits have lower total *REE* contents (Table 6) and are relatively depleted in *LREE* (Figs. 14d, e, f). The lower total *REE* contents, lack of sulfides, and the strong fractionation between *LREE* and *HREE* are consistent with formation of these deposits under less reducing conditions wherein reduction of the oxidizing basinal brine occurred during interaction with the basement rocks, with minimal contribution of basement-derived fluid (Fig. 15). The moderate to high *REE* contents of uranium-mineralized rocks and associated clay alteration, and the low *REE* contents of unmineralized sandstones and basement rocks, imply that during diagenesis and formation of unconformity-type uranium deposits, the *REE* were remobilized from sandstones and basement rocks and concentrated in hydrothermal phosphate, silicate, clay, and uranium minerals.

### *Rare-earth-element and U mobility in the Athabasca Basin*

Although the rare-earth elements and Y are generally considered immobile, the results of many studies suggest that these elements can be mobile in hydrothermal solutions associated with many mineral deposits, including hydrothermal U–*REE* deposits (Perhac & Heinrich 1964, van Wambeke 1977, McLennan & Taylor 1979, Drysdall *et al.* 1984, Metz *et al.* 1985, Fryer & Taylor 1987, Kwak & Abeysinghe 1987, Trueman *et al.* 1988, Quirt *et al.* 1991). In most rock-forming and accessory minerals, the *REE* fill structural sites in eight-fold coordination and readily substitute for $Ca^{2+}$ and $Na^{+}$. The resulting charge-imbalance restricts the entry

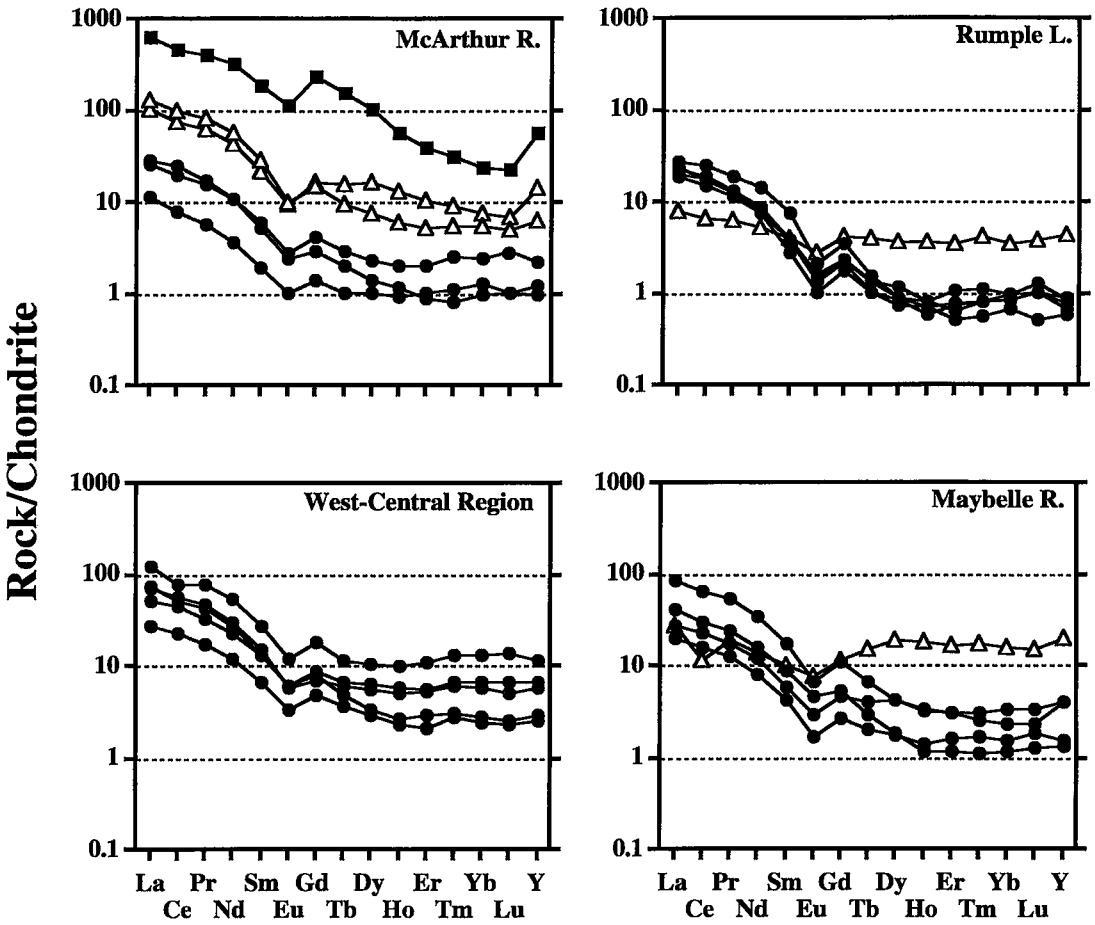


FIG. 13. Chondrite-normalized *REE* patterns for unmineralized sandstone, alteration halo associated with uranium minerals, and basement rocks from several localities from the Athabasca Basin (data from Table 5). Symbols: -●- unmineralized sandstone, -■- alteration halo, and -△- basement gneisses.

of *REE* into common rock-forming minerals, so that zircon, apatite, monazite, xenotime, a crandallite-group mineral, and garnet tend to concentrate the *REE* (Grauch 1989, McLennan 1989, Pan & Fleet 1996). Phosphate minerals (including fluorapatite), zircon, and garnet can contain up to 20 wt% $REE_2O_3$ (Rønsbo 1989), 10 wt% $REE_2O_3$ (Speer 1982) and 1 wt% $REE_2O_3$ (Jaffe 1951, Wakita *et al.* 1969, Meagher 1982), respectively. In addition, phosphate minerals and zircon can contain up to 0.5 wt% uranium (Speer 1982).

The relations among *REE*-rich minerals, diagenetic clays and uranium mineralization in the basin and basement rocks indicate U and *REE* mobility during peak diagenesis of the Athabasca Basin and subsequent episodes of uranium mineralization. The *REE* and U most likely were derived from detrital fluorapatite and zircon in the sandstone, garnet in basement rocks and, to a lesser extent, from diagenetic clay minerals in the sandstone and zircon in basement rocks. Diagenesis of the Athabasca Group clastic sediments at approximately 1500 Ma produced a highly saline (>100 000 mg/L solutes) oxidizing basinal fluid with a pH of about 6, which interacted with the Athabasca sandstone and formed the basin-wide assemblage of clays and silicates at temperatures of 200°C (Kotzer & Kyser 1995). Under these conditions, fluorapatite readily alters to an F-poor crandallite-group mineral (Cook 1970, Nriagu 1976), thus releasing the *HREE*, $HPO^{2-}_4$ and $F^-$ into the oxidizing basinal brine. The *LREE*, including $Ce^{4+}$, are incorporated in crandallite-group minerals:

$(Ca,REE)_5(PO_4)_3F + 3Al(OH)^-_4 + 12H^+ = (Ca,LREE)Al_3(PO_4)_2(OH) + 11(H_2O) + 4Ca^+ + HPO^{2-}_4 + F^- + HREE.$

TABLE 6. REE CONCENTRATIONS OF REPRESENTATIVE SAMPLES OF URANINITE, PITCHBLENDE, COFFINITE, AND Ca-U-HYDRATE MINERALS FROM THE ATHABASCA BASIN

| | Sue Zone | | Key L. | | McArthur R. | | Eagle Pt. (N and S) | | | Cigar L. |
|---|---|---|---|---|---|---|---|---|---|---|
| DDH | 528 | 528 | 487 | 487 | 204 | 204 | 779 | 779 | 213 | 480 |
| Depth (m) | 129 | 129 | 14 | 14 | 503 | 503 | 57(N) | 57(N) | 224(S) | 176 |
| Element | pitch. | Ca-U | uran. | coff. | uran. | coff. | uran. | Ca-U | Ca-U | pitch. |
| Th | 26.0 | 23.4 | 43.4 | 63.8 | 5.9 | 7.3 | 1.4 | 13.7 | 21.5 | 59.0 |
| La | 2.1 | 0.70 | 214 | 126 | 54.9 | 25.1 | 42.4 | 29.0 | 107 | 872 |
| Ce | 9.2 | 4.1 | 982 | 497 | 156 | 47.3 | 105 | 92.7 | 211 | 3638 |
| Pr | 1.3 | 0.60 | 141 | 65.2 | 32.0 | 7.6 | 19.9 | 16.5 | 35.3 | 410 |
| Nd | 7.9 | 2.9 | 618 | 286 | 214 | 52.4 | 115 | 86.4 | 166 | 1633 |
| Sm | 11.3 | 5.5 | 385 | 123 | 254 | 51.0 | 83.3 | 51.4 | 66.7 | 285 |
| Eu | 5.9 | 3.2 | 129 | 38.9 | 115 | 23.2 | 33.2 | 22.0 | 19.9 | 103 |
| Gd | 84.3 | 44.7 | 772 | 203 | 777 | 181 | 170 | 112 | 105 | 714 |
| Tb | 60.0 | 32.5 | 250 | 61.0 | 230 | 49.8 | 65.9 | 43.3 | 43.6 | 170 |
| Dy | 489 | 266 | 1379 | 330 | 1386 | 297 | 578 | 366 | 387 | 953 |
| Ho | 66.0 | 37.2 | 169 | 41.2 | 194 | 43.6 | 87.5 | 52.4 | 58.6 | 122 |
| Er | 135 | 74.5 | 351 | 82.1 | 413 | 95.0 | 198 | 115 | 124 | 245 |
| Tm | 15.3 | 8.5 | 39.5 | 10.4 | 47.3 | 12.4 | 23.9 | 15.4 | 17.2 | 28.1 |
| Yb | 80.7 | 46.2 | 231 | 63.3 | 270 | 66.0 | 138 | 82.9 | 93.1 | 157 |
| Lu | 7.4 | 4.1 | 20.2 | 5.2 | 27.3 | 8.4 | 13.0 | 7.0 | 8.6 | 15.8 |
| Y | 922 | 562 | 1875 | 536 | 2921 | 847 | 1349 | 813 | 880 | 2428 |
| Total | 1897 | 1093 | 7555 | 2468 | 7092 | 1807 | 3022 | 1906 | 2323 | 11774 |
| Total LREE | 31.9 | 13.8 | 2341 | 1097 | 711 | 183 | 365 | 276 | 585 | 6839 |
| Total HREE | 937 | 514 | 3211 | 769 | 3345 | 753 | 1275 | 795 | 837 | 2404 |
| HREE/LREE | 29.4 | 37.2 | 1.4 | 0.70 | 4.7 | 4.1 | 3.5 | 2.8 | 1.4 | 0.35 |

Note: all values are reported in ppm
Abbreviations: pitch.=pitchblende; uran.=uraninite; coff.=coffinite; Ca-U=Ca-U-hydrate minerals; DDH=diamond drill hole; N=north; S=south; L.=Lake; R.=River.

Zircon, in the presence of an oxidizing F-rich, neutral to alkaline fluid, is highly soluble (Saxena 1966, Kraynov 1969, Giere 1989, Rubin *et al.* 1993). In addition, the oxidizing nature of the basinal brine readily causes conversion of $U^{4+}$ in zircon to $U^{6+}$, which is highly soluble (Grandstaff 1976, Bruno *et al.* 1991). Therefore, detrital zircon was easily dissolved by the oxidizing, F-rich basinal brine, thus releasing *HREE* and U into solution. The basinal brine was enriched in *HREE* and $U^{6+}$, and depleted in *LREE*, which were incorporated in diagenetic crandallite-group minerals.

The 200°C reducing basement-derived fluid carried dissolved sulfides, and altered *REE*-rich minerals such as Mg–Ca-bearing garnet, to Al–Mg-bearing chlorite and fluorapatite, thereby releasing the *REE* into solution. Under these conditions, zircon solubility is limited, and zircon was altered to xenotime. The basement-derived fluid, therefore, was enriched in *REE*. The presence of hydrothermal fluorapatite, xenotime, and a crandallite-group mineral implies that the basement fluid also was characterized by relatively high activities of F and P.

The interaction between the oxidizing basinal brine and reducing basement rocks sufficiently changed the physicochemical characteristics of the basinal brine and precipitated simple-type uranium minerals, which incorporated the *HREE* present in the brine and produced concave chondrite-normalized *REE* patterns (Figs. 13, 14). Mixing between oxidizing basinal brine and reducing basement-derived fluids similarly caused sufficient change in the physicochemical composition of both fluids and precipitated complex-type uranium minerals, which incorporated the *HREE* and *LREE* from both fluids and produced relatively flat, chondrite-normalized *REE* patterns. Experimental studies have shown that 20–95% of the *REE* in clay minerals are readily leachable and may be available for migration during diagenesis, the intermediate and heavy *REE* being most susceptible, and the *LREE* the least (Balashov & Girin 1969, Roaldset & Rosenqvist 1971, Clauer *et al.* 1993). During the subsequent basin-wide fluid-circulation events at ~950 Ma and 300 Ma, the *REE* may have been leached from early-diagenetic clay minerals and uranium minerals, in addition to any detrital phosphate minerals, zircon, and garnet remaining, and subsequently incorporated into newly formed uranium ore.

### *REE and U complexation and transport in the Athabasca Basin*

The *REE* can be transported by a number of inorganic complexes in solution, namely hydroxide, phosphate, carbonate, fluoride, chloride, sulfate, sulfur complexes, and several less important organic complexes (Brookins 1989, Wood 1990a, b, Haas *et al.* 1995). Theoretical predications by Wood (1990b) of *REE* speciation in hydrothermal solutions indicate that fluoride complexes dominate over other complexes, including chloride complexes, throughout the entire pH range at low ($10^{-4}$ m) and high ($10^{-2}$ m) fluoride concentrations and at temperatures of approximately 200°C. More recent studies by Haas *et al.* (1995) show that *REE* speciation is strongly sensitive to the pH of the fluid. At neutral pH, *REE*–fluoride complexes dominate over chloride and hydroxide complexes. The *HREE* (Gd–Lu) are complexed more strongly by fluoride, and less strongly by chloride, than the *LREE* (La–Sm) (Haas *et al.* 1995). Fluoride content of common types of brines ranges from 0.1 to 10 ppm (White *et al.* 1963).

During the diagenesis of the Athabasca Group, alteration of detrital fluorapatite to an F-poor crandallite-group mineral released F into the basinal brine. The pH of the fluid most likely was similar to the calculated pH (4.8 to 6.0) of fluids associated with uranium from unconformity-type uranium deposits in Australia (Komninou & Sverjensky 1995). In addition, the presence of hydrothermal fluorapatite in basement rocks indicates the presence of F in the basement fluid. The absence of hydrothermal or diagenetic fluorite in the Athabasca Basin implies that fluoride concentrations in the fluids were within the range where *REE*-fluoride complexes dominate. Therefore, the *REE* in the Athabasca Basin most likely were transported as fluoride complexes. At 200°C, pH in the range between 5 and 7, and a wide range in F activity, $LnF_3^0$ is predicted to be the dominant *REE*-fluoride complex (Wood 1990b). However, Bilal & Koss (1982) have measured stability constants for mixed *REE* hydroxofluoride complexes indicating that such mixed complexes may be important at low

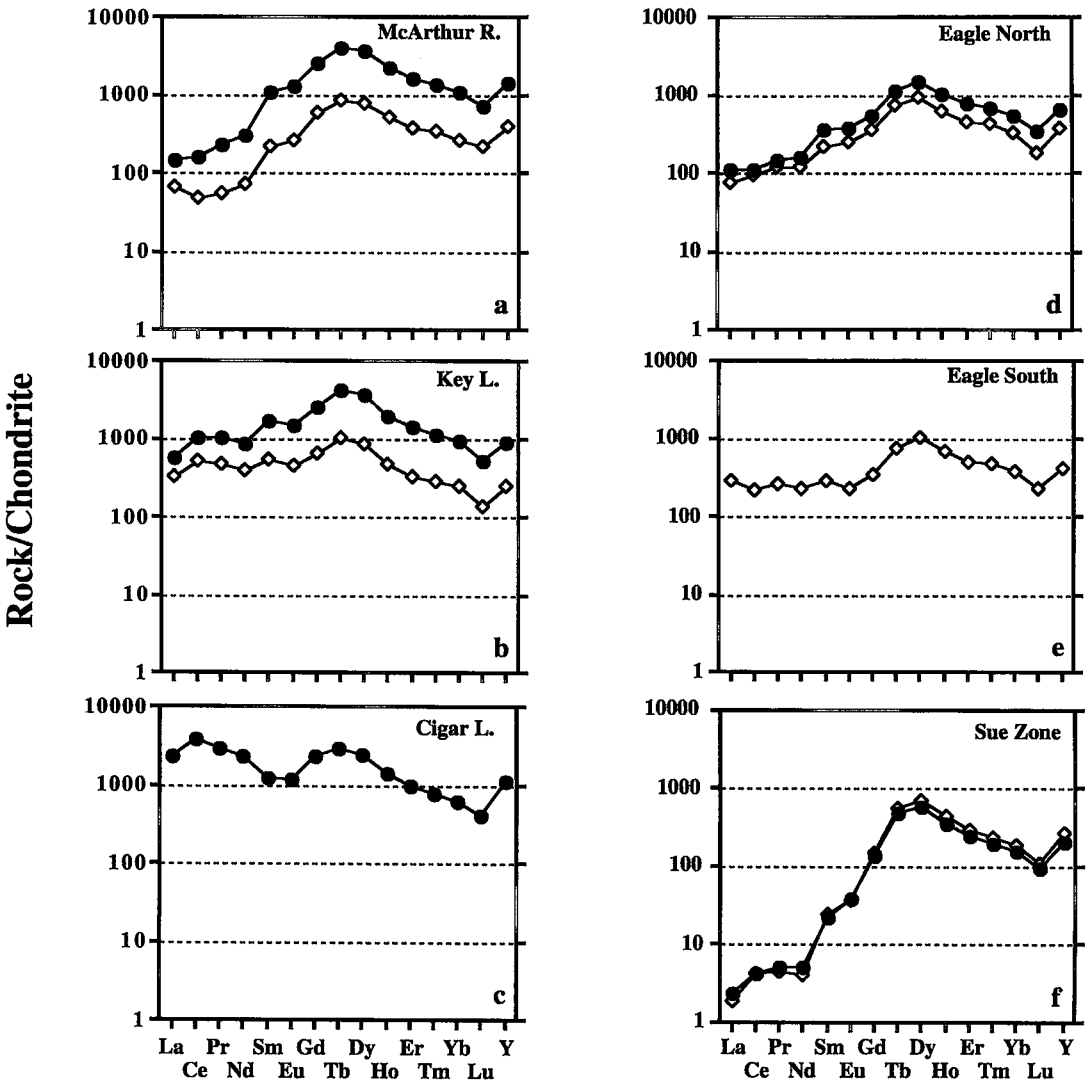


FIG. 14. Chondrite-normalized REE patterns for uraninite–pitchblende and "gummite"–coffinite from a) McArthur River, b) Key Lake, c) Cigar Lake, d) Eagle Point North, e) Eagle Point South, and f) Sue Zone (data from Table 6). Symbols: -●- uraninite–pitchblende, and -◇- "gummite"–coffinite.

fluoride activities and neutral pH. Therefore, mixed complexes may have been important in the transport of *REE* during subsequent fluid-flow events at 950 Ma and 300 Ma, where fluids had lower fluorine contents.

Uranium is generally transported as $U^{6+}$ because $U^{4+}$ is relatively insoluble (Grandstaff 1976, Romberger 1984). Calculations by Romberger (1984) on uranium speciation in 200°C fluids that contain 100 ppm F, 1000 ppm $SO_4$, 1 m NaCl, 1 ppm P, and $P(CO_2)$ of 1 atm indicate that $UO_2F_3^-$ complex would dominate at pH 4 to 6, whereas $UO_2(HPO_4)_2^{2-}$ would dominate at pH 6 to 8. The alteration of fluorapatite by the basinal fluid forming a crandallite-group mineral liberates both $F^-$ and $HPO_4^{2-}$ into solution. Therefore, uranium may be transported in the fluid as both uranium–phosphate and uranium–fluoride complexes. However, basinal brines from the Athabasca Basin have greater than 1 m NaCl concentrations (Kotzer & Kyser 1995), and under these conditions, uranyl–chloride complexes may be important in the transport of uranium (Wilde & Wall 1987). Therefore, during peak diagenesis of the Athabasca Basin at ~1500 Ma, U- and *REE*-fluoride complexes

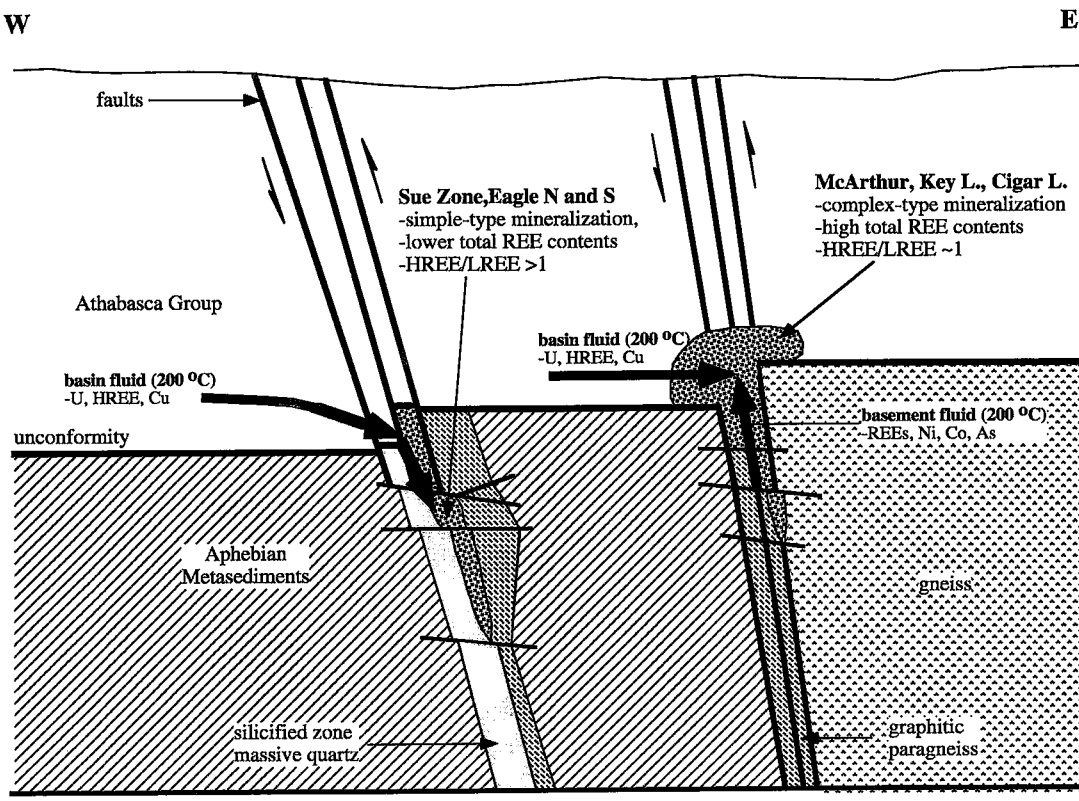


FIG. 15. Schematic cross-section of the two major types of unconformity-type uranium deposits found in the Athabasca Basin, showing a simplified pattern of circulation of basin- and basement-derived fluids.

were likely the dominant complexes in solution. However, phosphate and chloride complexes may have been dominant during subsequent fluid-circulation events, during which fluids had lower fluoride contents.

## FLUID–METAL BUDGET OF THE ATHABASCA BASIN

Presently, the Athabasca Basin is approximately 400 km long and 200 km wide, and the sedimentary sequence is approximately 2 km thick (Kotzer & Kyser 1995). However, temperature estimates from fluid inclusions indicate that the Athabasca sediments may have reached a thickness of 5–7 km in the mid-Proterozoic (Pagel *et al.* 1980), so that the volume of the Athabasca Basin could have been as great as 10,000 to 15,000 km$^3$. The porosity of the present-day Athabasca sedimentary sequence ranges from 2 to 20% (Winberg & Stevenson 1994), whereas during the mid-Proterozoic, prior to compaction, the porosity of the Athabasca sequence may have been as high as 30%. Therefore, if one assumes that all pore space was filled with fluid, the volume of fluid generated during diagenesis of the Athabasca Basin could have ranged from 1000 to 3000 trillion liters.

The concentration of uranium in sediments that were derived from uranium-rich granites and pegmatites is approximately 70 ppm (Macleod 1992). The source of the sediments in the Athabasca Basin is assumed to have been the Cree Lake zone and Wollaston Domain (Ramaekers 1979, Langford 1986), which contain uraniferous granitic pegmatites and subeconomic uranium showings (Thomas 1983, Giblin & Appleyard 1987). As such, we can assume that the uranium concentration in Athabasca sandstone prior to diagenesis was approximately 70 ppm, and that detrital zircon likely contained most of the uranium. Therefore, prior to diagenesis, the total amount of uranium in the Athabasca Group Sandstone sequences was approximately 1500 billion kilograms, assuming that the volume of the Athabasca Basin was 10 000 km$^3$, of which 20% was pore fluid. At present, unmineralized diagenetically altered sandstone has approximately 2 ppm uranium, and unconformity-type uranium deposits presently have an estimated geological reserve of 427 million kilograms of uranium. Therefore,

97% of the uranium was remobilized during fluid migration, but only 2% of the uranium was deposited in known unconformity-type uranium deposits. The rest of the uranium either remained in the fluid phase, or is incorporated in uranium deposits that have yet to be found.

The concentration of *REE* in sediments derived from granites is approximately 300 ppm, mostly held in phosphate and clay minerals (Mongelli 1993). Therefore, prior to diagenesis, the total *REE* content of the Athabasca Group sandstone sequence may have been *ca.* 6 trillion kilograms. At present, the *REE* concentration of unmineralized diagenetically altered sandstone is approximately 100 ppm. *REE* contents in uranium minerals range from 5000 to 12,000 ppm, so that the estimated geological reserve of *REE* associated with unconformity-type uranium deposits is approximately 5 million kilograms. Therefore, approximately 65% of the *REE* were mobilized during diagenesis and fluid migration, but only a very small fraction of the *REE* are associated with known uranium deposits. The solubility of aqueous *REE*-complexes is almost certainly independent of redox conditions. However, uranium will precipitate if the redox conditions of the fluid change and become reduced. Therefore, the mechanism that caused uranium to precipitate was likely not as efficient at destabilizing aqueous *REE*-complexes, and therefore most of the *REE* may have remained in solution.

More uranium was mobilized during diagenesis relative to *REE* because the diagenetic crandallite-group mineral (after detrital apatite), rutile, and hematite retained the *LREE* and some of *HREE*. However, detrital zircon (the main source of uranium) is soluble in diagenetic, oxidizing, F-rich, neutral to alkaline fluids (Saxena 1966, Kraynov *et al.* 1969, Gieré 1989, Rubin *et al.* 1993). Therefore, the oxidizing basinal brine could well have completely dissolved the detrital zircon, which liberated the uranium from the structure. As such, the basinal brine was much more efficient at mobilizing uranium relative to *REE*.

## Summary

1. Three main stages of uranium mineralization have been identified. Uranium minerals are chemically not homogeneous; most uraninite and pitchblende grains have variable U/Pb ratios and Si, Ca, and Fe contents that generally increase toward grain boundaries. The three stages of uranium mineralization are variably altered to "gummite" and coffinite, which have low but variable Pb contents and variable Si, Ca, and Fe contents.

2. The petrography of unmineralized sandstones, basement rocks, and clay-mineral alteration haloes associated with uranium mineralization indicates the presence of detrital, diagenetic and hydrothermal *REE*-phosphate and silicate minerals. Detrital fluorapatite in unmineralized sandstone and alteration haloes is altered to a crandallite-group mineral, whereas detrital zircon is altered to xenotime. Garnet in altered basement rocks is altered to hydrothermal fluorapatite and Al–Mg-bearing chlorite.

3. The least altered stage-1 and -2 uraninite and pitchblende, with the highest reflectivity, have the lowest $\delta^{18}O$ values. A positive correlation exists between $\delta^{18}O$ values and Si and Ca contents of uraninite, pitchblende, "gummite" and coffinite, because uranium minerals incorporated $^{18}O$-rich $SiO_2$ and CaO during formation or alteration; on the other hand, a negative correlation exists between $\delta^{18}O$ values and Pb contents, because uranium minerals with the highest Si and Ca contents and consequently the highest $\delta^{18}O$ values are the most altered and paragenetically late.

4. The low $\delta^{18}O$ values of relatively unaltered stage-1 and -2 uraninite and pitchblende, in conjunction with the theoretical uraninite–water fractionation-factors, indicate that the primary uranium mineralization is not in oxygen isotopic equilibrium with fluids that precipitated alteration minerals associated with primary uraninite and pitchblende. However, the assumptions used to derive the theoretical uraninite–water fractionation factors may not be appropriate for natural uraninite and pitchblende, and therefore, stage-1 and -2 uraninite and pitchblende may have partially retained their original oxygen isotopic composition.

5. The $^{207}Pb/^{206}Pb$ ages of uranium minerals are generally older than their chemical U–Pb ages and therefore suggest that radiogenic lead has been preferentially removed relative to uranium during the alteration of primary uranium minerals, a process supported by the young $^{207}Pb/^{206}Pb$ and U–Pb chemical ages of Ca-rich uranium hydrate minerals and coffinite.

6. The $^{87}Sr/^{86}Sr$ ratios of uranium minerals strongly reflect the proportion of basin and basement fluid involved in the formation of the deposits. Uranium minerals in simple-type deposits have $^{87}Sr/^{86}Sr$ ratios similar to those of illite from diagenetically altered sandstone, suggesting that the majority of the fluid involved in the formation of these deposits was basinal brine. In contrast, uranium minerals in complex-type deposits have higher $^{87}Sr/^{86}Sr$ ratios, similar to the clay minerals in altered basement rocks, and therefore a large proportion of the fluid involved in the formation of these deposits was derived from the basement rocks.

7. The *REE* contents of uraninite and pitchblende are as high as 12,000 ppm. Uranium minerals from complex-type deposits have the highest total *REE* contents and have relatively flat normalized *REE* patterns. The source of the *REE* was most likely both basin and basement fluids. In contrast, uranium minerals from simple-type deposits have lower total *REE* contents, more concave *REE* patterns, and the source of the *REE* was most likely the basinal brine.

8. The relations among detrital and diagenetic *REE*-rich minerals, diagenetic clays, and uranium minerals in the basin and basement rocks indicate extensive *REE* mobility during diagenesis of the Athabasca Basin and

episodes of uranium mineralization. In the presence of moderate concentrations (0.1 to 10 ppm) of fluorine in solution, *REE*- and U-fluoride complexes dominate over all other complexes over a wide range of pH and at 200°C. Therefore, the *REE* and U were most likely transported as fluoride complexes. Although uranium minerals in the Athabasca Basin have high *REE* contents, diagenetic and basement fluids were much more efficient at remobilizing uranium from the source than the *REE*.

## ACKNOWLEDGEMENTS

We thank CAMECO for logistical support in the field, and V. Sopuck and J. Marlatt for sharing their knowledge of the deposits' geology. Technical assistance provided by D. Pezderic and K. Klassen (stable isotopes), A. Vuletich, A. Bilanski, and C. Swiney (radiogenic isotopes), T. Bonli (electron microprobe), and B. Morgan (ICP–MS) was appreciated. Financial support was provided by the Natural Sciences and Engineering Research Council of Canada and CAMECO through a University–Industry Research Grant to T.K. Kyser. The manuscript benefitted greatly from the reviews by Bob Martin, Scott Wood, and Michel Cuney.

## REFERENCES

ARMSTRONG, R.L. & RAMAEKERS, P. (1985): Sr isotopic study of Helikian sediment and diabase dikes in the Athabasca Basin, northern Saskatchewan. *Can. J. Earth Sci.* **22**, 399-407.

BAADSGAARD, H. CUMMING, G.L. & WORDEN, J.M. (1984): U–Pb geochronology of minerals from the Midwest uranium deposit, northern Saskatchewan. *Can. J. Earth Sci.* **21**, 642-648.

BALASHOV, Y.A. & GIRIN, Y.P. (1969): On the reserve of mobile rare earth elements in sedimentary rocks. *Geochem. Int.* **6**, 649-659.

BERMAN, R.M. (1957): The role of lead and excess oxygen in uraninite. *Am. Mineral.* **42**, 705-731.

BILAL, B.A. & KOSS, V. (1982): Complex formation of trace elements in geochemical systems. VI. Study on the formation of hydroxo fluoro mixed ligand complexes of the lanthanide elements in a fluorite bearing system. *Polyhedron* **1**, 239-241.

BOWLES, J.F.W. (1990): Age dating of individual grains of uraninite in rocks from electron microprobe analyses. *Chem. Geol.* **83**, 47-53.

BRANDT, S.B. & PERMINOV, A.V. (1968): P–T dependence of migration properties of lead under hydrothermal conditions. *Geochem. Int.* **5**, 614-617.

BROOKINS, D.G. (1989): Aqueous geochemistry of rare earth elements. *In* Geochemistry and Mineralogy of Rare Earth Elements (B.R. Lipin & G.A. McKay, eds.). *Rev. Mineral.* **21**, 201-225.

BRUNETON, P. (1993): Geological environment of the Cigar Lake uranium deposit. *Can. J. Earth Sci.* **30**, 653-673.

BRUNO, J., CASAS, I. & PUIGDOMÈNECH, I. (1991): The kinetics of dissolution of $UO_2$ under reducing conditions and the influence of an oxidized surface layer ($UO_{2+x}$): application of a continuous flow-through reactor. *Geochim. Cosmochim. Acta* **55**, 647-658.

BURNS, P.C., MILLER, M.L. & EWING, R.C. (1996): $U^{6+}$ minerals and inorganic phases: a comparison and hierarchy of crystal structures. *Can. Mineral.* **34**, 845-880.

CARL, C., HÖHNDORF, A., VON PECHMANN, E., STRNAD, J.G. & RUHRMANN, G. (1988): Geochronology of the Key Lake uranium deposit, Saskatchewan, Canada. *Chem. Geol.* **70**, 133 (abstr.).

_____, VON PECHMANN, E., HÖHNDORF, A. & RUHRMANN, G. (1992): Mineralogy and U/Pb, Pb/Pb and Sm/Nd geochronology of the Key Lake uranium deposit, Athabasca Basin, Saskatchewan, Canada. *Can. J. Earth Sci.* **29**, 879-895.

CLAUER, N., CHAUDHURI, S., KRALIK, M. & BONNOT-COURTOIS, C. (1993): Effects of experimental leaching on Rb–Sr and K–Ar isotopic systems and *REE* contents of diagenetic illite. *Chem. Geol.* **103**, 1-16.

CLAYTON, R. & MAYEDA, T.K. (1963): The use of bromine pentafluoride in the extraction of oxygen from oxides and silicates for isotopic analysis. *Geochim. Cosmochim. Acta* **27**, 43-52.

COOK, P.J. (1970): Repeated diagnetic calcitization, phosphatization, and silicification in the Phosphoria Formation. *Geol. Soc. Am., Bull.* **81**, 2107-2116.

CUMMING, G.L. & KRSTIC, D. (1992): The age of unconformity-related uranium mineralization in the Athabasca Basin, northern Saskatchewan. *Can. J. Earth Sci.* **29**, 1623-1639.

DEER, W.A., HOWIE, R.A. & ZUSSMAN, J. (1992): *An Introduction to the Rock-Forming Minerals* (2nd ed.). Longman Scientific and Technical, Hong Kong.

DRYSDALL, A.R., JACKSON, N.J., RAMSAY, C.R., DOUCH, C.J. & HACKETT, D. (1984): Rare element mineralization related to Precambrian alkali granites in the Arabian Shield. *Econ. Geol.* **79**, 1366-1377.

DYCK, W. (1978): The mobility and concentration of uranium and its decay products in temperate surficial environments. *In* Uranium Deposits: their Mineralogy and Origin (M.M. Kimberley, ed.). *Mineral. Assoc. Can., Short-Course Vol.* **3**, 57-91.

EY, F., PIQUARD, J.P. & ZIMMERMAN, J. (1991): The Sue uranium deposits, Saskatchewan, Canada. *In* The Geological Society of CIM; first annual field conference (I.A. Homeniuk, ed.), 35-36.

FAYEK, M. & KYSER, T.K. (1993): Petrography, chemical ages, stable isotopic compositions, and *REE* contents of three

stages of uranium mineralization from the Athabasca Basin. *Saskatchewan Geol. Surv., Summary of Investigations* **1993**, 166-173.

FLEET, M.E. & PAN, YUANMING (1995): Crystal chemistry of rare earth elements in fluorapatite and some calc-silicates. *Eur. J. Mineral.* **7**, 591-605.

FRYER, B. & TAYLOR, R.P. (1987): Rare-earth element distributions in uraninites: implications for ore genesis. *Chem. Geol.* **63**, 101-108.

GIBLIN, A.M. & APPLEYARD, E.C. (1987): Uranium mobility in non-oxidizing brines: field and experimental evidence. *Appl. Geochem.* **2**, 285-295.

GIERÉ, R. (1989): Hydrothermal mobility of Ti, Zr and *REE*: examples from the Bergall and Adamello contact aureoles (Italy). *Terra Nova* **2**, 60-67.

GRANDSTAFF, D.E. (1976): A kinetic study of the dissolution of uraninite. *Econ. Geol.* **71**, 1493-1506.

GRAUCH, R.I. (1989): Rare earth elements in metamorphic rocks. *In* Geochemistry and Mineralogy of Rare Earth Elements (B.R. Lipin & G.A. McKay, eds.). *Rev. Mineral.* **21**, 147-167.

HAAS, J.R., SHOCK, E.L. & SASSANI, D.C. (1995): Rare earth elements in hydrothermal systems: estimates of standard partial molal thermodynamic properties of aqueous complexes of the rare earth elements at high pressures and temperatures. *Geochim. Cosmochim. Acta* **59**, 4329-4350.

HATTORI, K. & HALAS, S. (1982): Calculation of oxygen isotope fractionation between uranium dioxide, uranium trioxide and water. *Geochim. Cosmochim. Acta* **46**, 1863-1868.

_____, MUEHLENBACHS, K. & MORTON, D. (1978): Oxygen isotope geochemistry of uraninites. *Geol. Soc. Am. – Geol. Assoc. Can. – Mineral. Assoc. Can., Program Abstr.* **10**, A417.

HOEKSTRA, H.R. & KATZ, J.J. (1955): Isotope geology of some uranium minerals. *U.S. Geol. Surv., Prof. Pap.* **300**, 543-547.

HOEVE, J., CUMMING, G.L., BAADSGAARD, H. & MORTON, R.D. (1985): Geochronology of uranium metallogenesis in Saskatchewan. *In* Geology of Uranium Deposits (T.I.I. Sibbald & W. Petruk, eds.). *Can. Inst. Mining Metall., Spec. Vol.* **32**, 56-63.

_____ & QUIRT, D. (1984): Mineralization and host rock alteration in relation to clay mineral diagenesis and evolution of the middle-Proterozoic Athabasca Basin, northern Saskatchewan, Canada. *Sask. Res. Council, Tech. Rep.* **187**.

_____ & SIBBALD, T. (1978): On the genesis of Rabbit Lake and other unconformity-type uranium deposits in northern Saskatchewan, Canada. *Econ. Geol.* **73**, 1450-1473.

_____, _____, RAMAEKERS, P. & LEWRY, J.F. (1980): Athabasca Basin unconformity-type uranium deposits: a special class of sandstone-type deposits. *In* Uranium in the Pine Creek Geosyncline (J. Ferguson & A.B. Goleby, eds.). Int. Atomic Energy Agency (Vienna), 575-594.

HÖHNDORF, F., LENZ, H., VON PECHMANN, E., VOULTSIDIS, V. & WENDT, I. (1985): Radiometric age determinations on samples of Key Lake uranium deposits. *In* Geology of Uranium Deposits (T.I.I. Sibbald & W. Petruk, eds). *Can. Inst. Mining Metall., Spec. Vol.* **32**, 48-53.

JAFFE, H.W. (1951): The role of yttrium and other minor elements in the garnet group. *Am. Mineral.* **36**, 133-155.

KNIPPING, H.D. (1974): The concepts of supergene versus hypogene emplacement of uranium at Rabbit Lake, Saskatchewan, Canada. *In* Formation of Uranium Ore Deposits. Int. Atomic Energy Agency (Vienna) **STI/P49/374**, 531-549.

KOMNINOU, A. & SVERJENSKY, D.A. (1995): Hydrothermal alteration and the chemistry of ore-forming fluids in an unconformity-type uranium deposit. *Geochim. Cosmochim. Acta* **59**, 2709-2723.

KOTZER, T.G. & KYSER, T.K. (1990a): The use of stable and radiogenic isotopes in the identification of fluids and processes associated with unconformity-type uranium deposits. *In* Modern Exploration Techniques (L.S. Beck & C.T. Harper, eds.). *Sask. Geol. Soc., Spec. Publ.* **10**, 115-131.

_____ & _____ (1990b): Fluid history of the Athabasca Basin and its relation to uranium deposits. *In* Summary of investigations 1990. *Sask. Geol. Surv., Misc. Rep.* **90-4**, 153-157.

_____ & _____ (1992): Isotopic, mineralogic and chemical evidence for multiple episodes of fluid movement during prograde and retrograde diagenesis in a Proterozoic Basin. *In* Proc. 7th Int. Symp. on Water–Rock Interaction (Y.K. Kharaka & A.S. Maest, eds.). 1177-1181.

_____ & _____ (1993): O, U and Pb isotopic and chemical variations in uraninite: implications for determining the temporal and fluid history of ancient terrains. *Am. Mineral.* **78**, 1262-1274.

_____ & _____ (1995) Petrogenesis of the Proterozoic Athabasca Basin, northern Saskatchewan, Canada, and its relation to diagenesis, hydrothermal uranium mineralization and paleohydrogeology. *Chem. Geol.* **120**, 45-89.

KRAYNOV, S.T., MER'KOV, A.N., PETROVA, N.G., BATURINSKAYA, I.V. & ZHARIKOVA, V.M. (1969): Highly alkaline (pH 12) fluosilicate waters in the deeper zones of the Lovozero massif. *Geochem. Int.* **6**, 635-640.

KWAK, T.A.P. & ABEYSINGHE, P.B. (1987): Rare earth and uranium minerals present as daughter crystals in fluid inclusions, Mary Kathleen U–*REE* skarn, Queensland, Australia. *Mineral. Mag.* **51**, 665-670.

KYSER, T.K., KOTZER, T.G. & SIBBALD, T.I.I. (1990): Oxygen, U–Pb and Pb–Pb isotope systematics in uraninite from complex U–Au–PGE vein-type and unconformity-type U deposits in northern Saskatchewan. *In* Summary of investigations 1990. *Saskatchewan Geol. Surv., Misc. Rep.* **90-4**, 64-69.

_____, WILSON, M.R. & RUHRMANN, G. (1988): Stable isotopic constraints on the role of graphite in the genesis of unconformity-type uranium deposits. *Can. J. Earth Sci.* **26**, 490-498.

LANGFORD, F.F. (1974): Surficial origin of North American pitchblende and related uranium deposits. *Am. Assoc. Petroleum Geol., Bull.* **61**, 28-42.

_____ (1986): Geology of the Athabasca Basin. *In* Uranium Deposits of Canada (E.L. Evans, ed.). *Can. Inst. Mining Metall., Spec. Vol.* **33**, 123-133.

LEWRY, J.F. & SIBBALD, T.I.I. (1977): Variation in lithology and tectonometamorphic relationships in the Precambrian basement of northern Saskatchewan. *Can. J. Earth Sci.* **14**, 1453-1467.

_____ & _____ (1980): Thermotectonic evolution of the Churchill Province in northern Saskatchewan. *Tectonophys.* **68**, 45-82.

_____, _____ & SCHELEDEWITZ, D.C.P. (1985): Variation in character of Archean rocks in the Western Churchill Province and its significance. *In* Evolution of Archean Supracrustal Sequences (L.D. Ayres, P.C. Thurston, K.D. Card & W. Weber, eds.). *Geol. Assoc. Can., Spec. Pap.* **28**, 239-261.

LONGERICH, H.P., JENNER, G.A., FRYER, B.J. & JACKSON, S.E. (1990): Inductively coupled plasma – mass spectrometric analysis of gelogical samples: a critical evaluation based on case studies. *Chem. Geol.* **83**, 105-118.

LUDWIG, K.R. (1993): ISOPLOT. A plotting and regression program for radiogenic-isotope data. *U.S. Geol. Surv., Open-File Rep.* **91-445**.

MACDONALD, R. (1987): Update on the Precambrian geology and domainal classification of northern Saskatchewan. *In* Summary of Investigations 1987. *Saskatchewan Geol. Surv., Misc. Rep.* **87-4**, 87-104.

MACLEOD, R. (1992): *Hydrogeological and Geochemical Controls on Trace Metal Concentrations in Lake Sediments in the Holyrood Granite.* M.Sc. thesis, Memorial Univ. of Newfoundland, St. John's, Newfoundland.

MARLATT, J., MCGILL, B., MATTHEWS, R., SOPUCK, V. & POLLOCK, G. (1992): The discovery of the McArthur River uranium deposit, Saskatchewan, Canada. *In* The Geological Society of CIM; first annual field conference (I.A. Homeniuk, ed.), 118-127.

MCLENNAN, S.M. (1989): Rare earth elements in sedimentary rocks: influence of provenance and sedimentary processes. *In* Geochemistry and Mineralogy of Rare Earth Elements (B.R. Lipin & G.A. McKay, eds.). *Rev. Mineral.* **21**, 169-200.

_____ & TAYLOR, S.R. (1979): Rare earth element mobility associated with uranium mineralization. *Nature* **282**, 247-249.

MEAGHER, E.P. (1982): Silicates garnets. *In* Orthosilicates (P.H. Ribbe, ed.). *Rev. Mineral.* **5**, 25-66.

METZ, M.C., BROOKINS, D.G., ROSENBERG, P.E. & ZARTMAN, R.E. (1985): Geology and geochemistry of the Snowbird deposit, Mineral County, Montana, *Econ. Geol.* **80**, 394-409.

MONGELLI, G. (1993): *REE* and other trace elements in a granitic weathering profile from "Serre", southern Italy. *Chem. Geol.* **103**, 17-25.

NRIAGU, J.O. (1976): Phosphate–clay mineral relations in soils and sediments. *Can. J. Earth Sci.* **13**, 717-736.

O'NEIL, J.R. (1986): Theoretical and experimental aspects of isotope fractionation. *In* Stable Isotopes in High Temperature Geological Processes (J.W. Valley, H.P. Taylor, Jr. & J.R. O'Neil, eds.). *Rev. Mineral.* **16**, 1-40.

PAGEL, M., MICHARD, A., JUTEAU, M. & TURPIN, L. (1993): Sm–Nd, Pb–Pb, and Rb–Sr systematics of the basement in Cigar Lake area, Saskatchewan, Canada. *Can. J. Earth Sci.* **30**, 731-742.

_____, POTY, B. & SHEPPARD, S.M.F. (1980): Contributions to some Saskatchewan uranium deposits mainly from fluid inclusion and isotopic data. *In* Uranium in the Pine Creek Geosyncline (J. Ferguson & A.B. Goleby, eds.). Int. Atomic Energy Agency (Vienna), 639-654.

PAN, YUANMING & FLEET, M.E. (1996): Intrinsic and extrinsic controls on the incorporation of rare-earth elements in calc-silicate minerals. *Can. Mineral.* **34**, 147-159.

PARRISH, R.R., RODDICK, J.C., LOVERIDGE, W.D. & SULLIVAN, R.W. (1987): Uranium–lead analytical techniques at the geochronology laboratory, Geological Survey of Canada. *In* Radiogenic Age and Isotopic Studies, Report 1. *Geol. Surv. Can., Pap.* **87-2**, 3-7.

PERCIVAL, J.B., BELL, K. & TORRANCE, J.K. (1993): Clay mineralogy and isotope geochemistry of the alteration halo at the Cigar Lake uranium deposit. *Can. J. Earth Sci.* **30**, 689-704.

PERHAC, R.M. & HEINRICH, E.W. (1964): Fluorite–bastnaesite deposits of the Gallinas Mountains, New Mexico, and bastnaesite paragenesis. *Econ. Geol.* **59**, 226-239.

POWERS, L. & STAUFFER, M. (1985): Multigeneration pitchblende from the Midwest uranium–nickel deposit, northern Saskatchewan. *Can. J. Earth Sci.* **25**, 1945-1954.

QUIRT, D., KOTZER, T.G. & KYSER, T.K. (1991): Tourmaline, phosphate minerals, zircon and pitchblende in the Athabasca group: Maw Zone and McArthur River areas, Saskatchewan. *In* Summary of investigations 1991. *Saskatchewan Geol. Surv., Misc. Rep.* **91-4**, 181-191.

RAMAEKERS, P. (1979): Stratigraphy of the Athabasca Basin. Summary of Investigations 1979. *Saskatchewan Geol. Surv., Misc. Rep.* **79-10**, 154-160.

_____ (1981): Hudsonian and Helikian basins of the Athabasca Region, northern Saskatchewan. *In* Proterozoic Basins of Canada (F.H.A. Campbell, ed.). *Geol. Surv. Can., Pap.* **81-10**, 219-233.

_____ & DUNN, C.D. (1977): Geology and geochemistry of the eastern margin of the Athabasca Basin. *Saskatchewan Geol. Soc., Spec. Publ.* **3**, 297-322.

REES, M.I. (1992): *History of the Fluids Associated with the Lode-Gold Deposits, and Complex U–PGE–Au Vein-Type Deposits, Goldfields Peninsula, Northern Saskatchewan, Canada.* M.Sc. thesis, Univ. of Saskatchewan, Saskatoon, Saskatchewan.

ROALDSET, E. & ROSENQVIST, I.T. (1971): Unusual lanthanide distribution. *Nature Phys. Sci.* **231**, 153-154.

ROBINSON, P., HIGGINS, N.C. & JENNER, G.A. (1986): Determination of rare-earth elements, yttrium and scandium in rocks by an ion exchange – X-ray fluorescence technique. *Chem. Geol.* **55**, 121-137.

ROMBERGER, S.B. (1984): Transport and deposition of uranium in hydrothermal systems of temperatures up to 300°C: geological implications. *In* Uranium Geochemistry, Resources (B. de Vivo, F. Ippolito, G. Capaldi & P.R. Simpson, eds.). The Institution of Mining and Metallurgy, London, U.K. (12-17).

RØNSBO, J.G. (1989): Coupled susbstitutions involving *REE*s and Na and Si in apatites in alkaline rocks from the Ilímaussaq intrusion, South Greenland, and the petrological implications. *Am. Mineral.* **74**, 896-901.

RUBIN, J.N., HENRY, C.D. & PRICE, J.G. (1993): The mobility of zirconium and other "immobile" elements during hydrothermal alteration. *Chem. Geol.* **110**, 29-47.

RUHRMANN, G. & VON PECHMANN, E. (1989): Structural and hydrothermal modification of the Gaertner uranium deposit, Key Lake, Saskatchewan, Canada. *In* Uranium Resources and Geology of North America. *Proc., Int. Atomic Energy Agency, Tech. Committee Meeting* (K.E. Muller, ed.), *Tech. Doc.* **500**, 363-377.

SAXENA, S.K. (1966): Evolution of zircons in sedimentary and metamorphic rocks. *Sedimentology* **6**, 1-33.

SMITH, D.K. (1984): Uranium mineralogy. *In* Uranium Geochemistry, Mineralogy, Geology, Exploration and Resources (B. de Vivo, F. Ippolito, G. Capaldi & P.R. Simpson, eds.). The Institution of Mining and Metallurgy, London, U.K. (43-88).

SPEER, J.A. (1982): Zircon. *In* Orthosilicates (P.H. Ribbe, ed.). *Rev. Mineral.* **5**, 67-112.

TAYLOR, S.R. & MCLENNAN, S.M. (1985): *The Continental Crust: its Composition and Evolution.* Blackwell, Oxford, U.K.

THOMAS, D.J. (1983): *Distribution, Geological Controls and Genesis of Uraniferous Pegmatites in the Cree Lake Zone of Northern Saskatchewan.* M.Sc. thesis, Univ. of Regina., Regina, Saskatchewan.

TRUEMAN, D.L., PEDERSEN, J.C., DE ST. JORRE, L. & SMITH, D.G.W. (1988): The Thor Lake rare-metal deposits, Northwest Territories. *In* Recent Advances in the Geology of Granite-Related Mineral Deposits (R.P. Taylor & D.F. Strong, eds.). *Can. Inst. Mining Metall., Spec. Pap.* **39**, 280-290.

URANIUM SASKATCHEWAN (1994): Uranium Saskatchewan, Fact Sheet **FS-9407**.

VAN WAMBEKE, L. (1977): The Karonge rare earth deposits, Republic of Burundi: new mineralogical–geochemical data and origin of the mineralization. *Mineral. Deposita* **12**, 373-380.

WAKITA, H., SHIBAO, K. & NAGASHIMA, K. (1969): Yttrian spessartine from Suishoyama, Fukushima Prefecture, Japan. *Am. Mineral.* **54**, 1678-1683.

WALLIS, R., SARACOGLU, N., BRUMMER, J. & GOLIGHTLY, J. (1983): Geology of the McClean uranium deposits. *Geol. Surv. Can., Pap.* **82-11**, 71-110.

WHITE, D.E., HEM, J.D. & WARING, G.A. (1963): Chemical composition of subsurface waters. *U.S. Geol. Surv., Prof. Pap.* 440-F.

WILDE, A.R. & WALL, V.J. (1987): Geology of the Nabarlek uranium deposit, Northern Territory, Australia. *Econ. Geol.* **82**, 1152-1168.

WILSON, J.A. (1985): The geology of the Athabasca Group in Alberta. *Alberta Res. Council Bull.* **49**.

WILSON, M.R. & KYSER, T.K. (1987): Stable isotope geochemistry of alteration associated with the Key Lake uranium deposit, Canada. *Econ. Geol.* **82**, 1540-1557.

WINBERG, A. & STEVENSON, D. (1994): Hydrogeological modelling. Atomic Energy Comm., Ltd., Final Rep., Cigar Lake Analog Study, **AECL-10851, COG-93-147, SKB TR 94-04**, 104-143.

WOOD, S.A. (1990a): The aqueous geochemistry of the rare-earth elements and yttrium. 1. Review of available low-temperature data for inorganic complexes and the inorganic *REE* speciation of natural waters. *Chem. Geol.* **82**, 159-186.

_____ (1990b): The aqueous geochemistry of the rare-earth elements and yttrium. 2. Theoretical predictions of speciation in hydrothermal solutions to 350°C at saturation water vapor pressure. *Chem. Geol.* **88**, 99-125.

XIE, Q., JAIN, J., SUN, M., KERRICH, R. & FAN, J. (1994): ICP–MS analysis of basalt BIR-1 for trace elements. *Geostandards Newsletter* **18**, 53-63.

YERSHOV, V.M. (1974): A method of examining the diffusion parameters of lead in uranium minerals. *Geokhimiya* **10**, 1565-1568 (in Russ.).

ZHENG, YONG-FEI (1991): Calculation of oxygen isotope fractionation in metal oxides. *Geochim. Cosmochim. Acta* **55**, 2299-2307.

*Received July 15, 1996, revised manuscript accepted March 7, 1997.*